Buffer-Aided Serial Relaying for FSO Communications: Asymptotic Analysis and Impact of Relay Placement

Chadi Abou-Rjeily, *Senior Member IEEE*, and Wissam Fawaz, *Senior Member IEEE*

***Abstract*—In this paper, we analyze multi-hop Free-Space Optical (FSO) communications in the context of decode-and-forward serial relaying where the relays are equipped with finite-size buffers. Based on a Markov chain analysis, we derive closed-form asymptotic expressions for the system outage probability (OP) and average packet delay (APD) for an arbitrary number of relays N_r and an arbitrary buffer size L. The closed-form evaluation links the system performance to the various network parameters in a simple and intuitive manner and it is useful for offering clear insights on the impact of the relay placement and the selection of the buffer size for practical FSO systems. We prove that buffer-aided multi-hop systems can reap a diversity gain that ranges from $\left\lceil \frac{N_r}{2} \right\rceil + 1$ to $N_r + 1$ compared to multi-hop buffer-free systems while the asymptotic APD values can range from N_r to $(L-1)N_r$ for $L \geq 2$. Our analysis also highlights on the optimal solutions capable of concurrently minimizing the OP and APD.**

***Index Terms*—Free space optics, multi-hop, relaying, buffer, asymptotic analysis, relay placement, diversity gain.**

I. Introduction

The high transmission capacity along with the cost-effective deployment associated with Free-Space Optical (FSO) communication makes the FSO technology an attractive solution to the "last mile" problem. This is motivated by the inherent ability of the license-free FSO links to connect end users to the ubiquitous wireline fiber optic infrastructure. Numerous other applications are also envisaged for FSO systems and they range from backhauling/fronthauling future 5G wireless communication networks to disaster recovery [1]. The problem of multi-hop communications, or serial relaying, has been well explored in the context of FSO communications [2]–[5]. Both amplify-and-forward (AF) [2], [3] and decode-and-forward (DF) [4], [5] relaying were considered whether in the context of non-coherent detection [3], [4] or coherent detection [2], [5]. The main advantage of serial relaying resides in extending the network coverage with a performance that is dominated by the weakest hop; i.e. the hop with the highest probability of failure (or outage probability). While the existing literature on FSO serial relaying revolves around buffer-free relays [2]–[5], numerous recent studies have shown that buffer-free systems overlook substantial performance gains that can be reaped from equipping the relays with buffers (or data queues). In fact, there has been a growing interest in buffer-aided (BA) relaying solutions whether in the context of radio-frequency (RF) systems [6]–[17] or FSO systems [18]–[21].

The problem of BA parallel relaying with RF systems was considered in [6]–[13]. The *max-link* relay selection protocol was proposed in [6] where, in a given time slot, a single relay (R) is selected to either receive from the source (S) or to transmit to the destination (D). In order to reduce the outage probability (OP), the activated link is selected among all available S-R and R-D links based on the availability of the channel state information (CSI). The *max-link* DF protocol was later extended to AF relaying in [7]. Several improvements on this protocol were proposed in [8]–[10] where in [8] the average packet delay (APD) was reduced by giving higher priority to the R-D links for the sake of emptying the relays' buffers at a faster pace. While the relay selection procedure in the *max-link* protocol is based on the CSI, buffer state information (BSI) was also considered by the relay selection scheme in [9]. In this reference, the relays were partitioned into three priority classes based on whether their buffers are full, empty or neither empty nor full. In addition to the CSI and BSI, [10] included the delay state information (DSI) as well where the packets delayed beyond a certain delay limit are dropped from the buffers. In addition, the *max-link* protocol was studied in [11] in the presence of source to destination direct connectivity, providing a framework encompassing both direct and relay-based source to destination data transfer. The possibility of direct source to destination connectivity was also considered in [12], where buffer-aided relaying was studied under delay constraints that took the form of delay violation probability limitation. Finally, the authors in [13] proposed a relay selection algorithm that effectively deals with outdated CSI.

BA-RF serial relaying was analyzed in [14]–[17]. The N_r-relay DF relaying scheme in [14], [15] was based on the transmission along the best hop in each time slot based on the CSI. It was observed that BA multi-hop relaying provides diversity gains without being able to quantify these gains since the derived OP lower bound did not possess the same slope as the exact OP. On the other hand, [16] tackled the problem of half-duplex multi-hop BA-RF relaying where the transmission rates of the nodes are adapted over the different fading blocks for the sake of maximizing the end-to-end average rate. Finally, [17] considered the problem of throughput maximization for two-hop BA-RF communications with a full-duplex relay. Adaptive transmission-reception is implemented at the relay depending on the state of the S-R and R-D links as well as

The authors are with the Department of Electrical and Computer Engineering of the Lebanese American University (LAU), Byblos, Lebanon. (e-mails: {chadi.abourjeily,wissam.fawaz}@lau.edu.lb).

on the level of self interference at the relay.

BA relaying with FSO and hybrid RF/FSO systems was considered in [18]–[21]. The scenario in [18] corresponds to a number of RF mobile users transmitting their information to a BA relay along the first hop while the relay multiplexes and retransmits the data to the destination along a hybrid RF/FSO link in the second hop. For this scenario, the link allocation problem was considered where the load can be split among the RF and FSO links. This study was then refined in [19], where an efficient mixed RF and hybrid FSO/RF network that makes the most of the high transmission rates of multiuser scenarios was introduced. On the other hand, the problem of BA relay selection with multiple relays was considered in [20] in the case of hybrid RF/FSO links where, therein, it was assumed that the buffers at the relays have an infinite size. Finally, the problem of BA-FSO parallel relaying was considered in [21] with multiple relays that are equipped with buffers having a finite size. A number of relaying protocols were investigated and compared in terms of the achievable OP and APD through a Markov chain analysis.

In this paper, we consider the problem of BA-FSO serial relaying with N_r relays in tandem (N_r+1 hops). The particularities of FSO transmissions render the BA serial relaying problem remarkably different from the corresponding problem pertaining to RF systems considered in [14]–[17]. In particular, FSO transceivers operate naturally in the full-duplex mode where simultaneous reception and transmission can take place at the photodetector and laser placed at each relay, respectively. Therefore, unlike the half-duplex RF schemes in [14]–[16], all nodes can be simultaneously activated (i.e. transmit and receive) in the FSO network without any co-channel interference. This alleviates the relay selection problem in [14], [15] where only a single-hop (the strongest one) is activated per time slot with only one node transmitting and another one receiving. In a similar manner, the half-duplexity constraint in [16] can be advantageously relaxed where this constraint imposes that node n must be in the silent mode if node $n+1$ is in the transmission mode. Obviously, this kind of constrained alteration between the different modes is not required in FSO networks. Similarly, the adaptive transmission/reception mode selection at the full-duplex BA RF relay is not required as in [17] since the self-interference, from which full-duplex RF relays suffer, is nonexistent at the FSO relays that are equipped with two optical transceivers each. Finally, unlike all existing BA serial relaying techniques in RF systems that require acquiring full CSI [14]–[17], this type of relaying can be efficiently implemented in the absence of CSI in the context of FSO communications.

The performance of the BA-FSO multi-hop system is evaluated analytically based on a Markov chain analysis where we determine the state transition matrix and the steady-state distribution leading to the evaluation of the OP and APD for any buffer size L. For dual-hop systems, we derive exact expressions for the OP and APD following from the possibility of solving for the steady-state distribution in this case. For (N_r+1)-hop systems (with $N_r \geq 2$), we derive asymptotic expressions for the OP and APD since the complexity of the problem renders the exact evaluation out of reach. The calculation methodology adopted in this case is based on the identification of a closed-subset of states that tends asymptotically to be an absorbing set. The concept of state lumping is then used to determine the steady-state distribution of the recurrent states of the closed-subset by linking the Markov chain of an n-hop network to the Markov chain of the simpler $(n-1)$-hop network. The asymptotic analysis shows that the performance is predominantly governed by the weakest hop. Denoting the index of this hop by $\tilde{n}$, we prove that the diversity gain with respect to buffer-free systems is equal to $N_r+1-\min\{\tilde{n}-1, N_r+1-\tilde{n}\}$ with an asymptotic APD value of $N_r+(L-2)(\tilde{n}-1)$ for $L \geq 2$.

While both BA parallel-relaying [21] and BA serial-relaying techniques are capable of boosting the reliability of the FSO network, serial-relaying presents the main advantage of extending the network coverage enabling the communication between two very distant source and destination nodes. In this context, the superiority of one scheme over the other is highly dependent on the network setup (mainly the positions of the relays) where in some scenarios parallel-relaying is better while in other scenarios serial-relaying is superior. Therefore, no solution is unconditionally better than the other and the system designer can opt to implement either one of these two options depending on the network parameters. In general, if the S-D distance is excessively long, it would be better to implement serial-relaying since, for a given relay, either the S-R link or the R-D link will be long resulting in a marginal improvement in the diversity order. In parallel-relaying FSO systems [21], the source and destination are equipped with N_r transceivers each while each one of the N_r relays is equipped with two transceivers. For the BA serial-relaying systems considered in this work, S and D need to be equipped with only one transceiver each while each one of the relays is equipped with two transceivers.

II. System Model and Preliminaries

A. Basic Parameters

1) Outage Probability: Consider an intensity-modulated with direct-detection (IM/DD) (N_r+1)-hop FSO system where the source (S) communicates with the destination (D) through N_r relays placed in series denoted by $\mathrm{R}_1,\ldots,\mathrm{R}_{N_r}$. For simplicity, S and D will be denoted by R_0 and R_{N_r+1}, respectively, and the length of the n-th hop between R_{n-1} and R_n will be denoted by d_n for $n=1,\ldots,N_r+1$. In this paper, we consider the scenario of DF relays each equipped with a buffer of size L packets. The system model is depicted in Fig. 1.

We consider the widely adopted FSO channel model encompassing the combined effects of gamma-gamma turbulence-induced fading and pointing errors [22] in the case of background noise limited receivers corrupted by white additive Gaussian noise. The outage probability along the n-th hop is related to the probability that the channel capacity along this hop falls below a certain threshold [6]. This probability

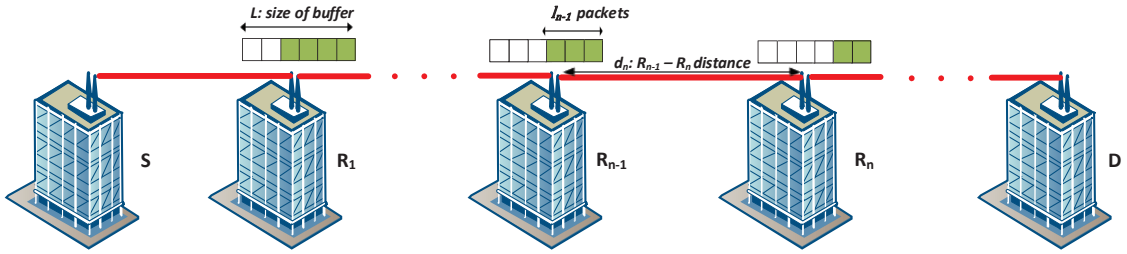

Fig. 1. Buffer-aided serial relaying FSO network.

can be determined from [23], [24] ($n = 1, \ldots, N_r + 1$):

$$p_n = \frac{\xi_n^2}{\Gamma(\phi_{1,n})\Gamma(\phi_{2,n})} \times G_{2,4}^{3,1}\left[\frac{\phi_{1,n}\phi_{2,n}}{G_n(P_M/(N_r+1))}\middle| \begin{matrix} 1, \xi_n^2+1 \\ \xi_n^2, \phi_{1,n}, \phi_{2,n}, 0 \end{matrix}\right], \quad (1)$$

where $G_{p,q}^{m,n}[\cdot]$ is the Meijer G-function and $\Gamma(\cdot)$ is the gamma function. In (1), P_M stands for the optical power margin that is normalized by $N_r + 1$ following from evenly splitting the power among the $N_r + 1$ hops where the considered multi-hop IM/DD FSO scheme can be implemented in the absence of CSI. In this context, binary pulse position modulation (PPM) can be implemented where the receiver decides in favor of the PPM slot with the maximum number of detected photons without the need for estimating the underlying channel irradiance [25]. This constitutes a major appealing feature for FSO communications that can be implemented in a simple manner. In (1), $\phi_{1,n} = \left[\exp\left(0.49\sigma_R^2(d_n)/(1+1.11\sigma_R^{12/5}(d_n))^{7/6}\right) - 1\right]^{-1}$ and $\phi_{2,n} = \left[\exp\left(0.51\sigma_R^2(d_n)/(1+0.69\sigma_R^{12/5}(d_n))^{5/6}\right) - 1\right]^{-1}$ stand for the parameters of the gamma-gamma distribution along the n-th hop where the distance-dependent Rytov variance is given by $\sigma_R^2(d) = 1.23C_n^2k^{7/6}d^{11/6}$ with k and C_n^2 denoting the wave number and refractive index structure parameter, respectively. In (1), the parameter ξ_n is related to the pointing errors and can be determined from $\xi_n = \omega_{z_{eq},n}/2\sigma_{s,n}$ where $\sigma_{s,n}$ stands for the pointing error displacement standard deviation at the receiver of R_n and $\omega_{z_{eq},n}^2 = \omega_{z,n}^2\sqrt{\pi}\mathrm{erf}(v_n)/[2v_ne^{-v_n^2}]$ [22]. In this last relation, $\omega_{z,n}$ stands for the beam waist along the n-th hop and $v_n = \sqrt{\pi/2}(a_n/\omega_{z,n})$ where a_n is the radius of the receiver at R_n while $\mathrm{erf}(\cdot)$ stands for the error function. Finally, G_n is a gain factor that follows since the n-th hop is shorter than the direct link S-D [24]:

$$G_n = e^{-\sigma(d_n - d_{\mathrm{SD}})}\frac{A_n}{A_{\mathrm{SD}}}\frac{\xi_{\mathrm{SD}}^2+1}{\xi_{\mathrm{SD}}^2}, \quad (2)$$

where σ is the attenuation coefficient and d_{SD} stands for the distance between S and D. Finally, $A_n = \mathrm{erf}^2(v_n)$ while A_{SD} and ξ_{SD} are the pointing error parameters associated with the link S-D.

The cooperative FSO network respects the same average and peak power constraints as in the conventional point-to-point noncooperative scenario. In fact, the power normalization by N_r+1 in (1) ensures that the average power transmitted by the N_r+1 nodes in the cooperative network is equal to the average power transmitted by the single node in the noncooperative scenario. Therefore, the achieved performance gains are not associated with any power penalty. Furthermore, reducing the amount of power transmitted by each node implies that the peak power constraint will be respected as well since even without this reduction (noncooperative case) the transmitted power is planned not exceed the values inflicted by the eye safety regulations.

2) Diversity Gain: For $P_M \gg 1$, p_n scales asymptotically as $p_n \to \left(\frac{a_nG_nP_M}{N_r+1}\right)^{-\beta_n}$ where $\beta_n = \min\{\phi_{2,n}, \xi_n^2\}$ and $a_n^{-\beta_n} = \frac{\xi_n^2(\phi_{1,n}\phi_{2,n})^{\beta_n}\Gamma(\phi_{1,n}-\beta_n)}{\Gamma(\phi_{1,n})\Gamma(\phi_{2,n})\beta_n}b_n$ where $b_n = 1/(\xi_n^2 - \phi_{2,n})$ if $\xi_n^2 > \phi_{2,n}$ and $b_n = \Gamma(\phi_{2,n} - \xi_n^2)$ if $\xi_n^2 < \phi_{2,n}$ [24] . The asymptotic expression of p_n reveals that the diversity and coding gains along the n-th hop are equal to β_n and $\frac{a_nG_n}{N_r+1}$, respectively.

The BA serial relaying scheme will be benchmarked against the corresponding buffer-free scheme [4] where the system will not suffer from outage only when all links are not in outage resulting in $P_{\mathrm{out}} = 1 - \prod_{n=1}^{N_r+1}(1-p_n)$. This relation can be approximated by $P_{\mathrm{out}} \approx \sum_{n=1}^{N_r+1} p_n \approx \max_{n=1,\ldots,N_r+1}\{p_n\} \triangleq p_{\tilde{n}}$ for asymptotically large values of P_M (resulting in small values of $\{p_n\}$) showing that the performance is dominated asymptotically by the weakest hop:

$$\tilde{n} = \arg\max_{n=1,\ldots,N_r+1}\{p_n\}. \quad (3)$$

Since the diversity gain β_n has a more prominent effect on p_n compared to the coding gain $\frac{a_nG_n}{N_r+1}$ (since β_n affects the slope of the OP curve), then for asymptotically large values of P_M, the highest outage probability p_n is associated with the smallest diversity gain β_n. Consequently, from (3), the asymptotic OP of the buffer-free scheme can be written as:

$$\max_{n=1,\ldots,N_r+1}\{p_n\} = p_{\tilde{n}} \to \left(\frac{a_{\tilde{n}}G_{\tilde{n}}P_M}{N_r+1}\right)^{-\beta}; \quad \beta \triangleq \beta_{\tilde{n}} = \min\{\beta_1, \ldots, \beta_{N_r+1}\}, \quad (4)$$

showing that the end-to-end diversity order is equal to β.

B. Buffer-Aided FSO Serial Relaying

The FSO relays operate naturally in the full duplex mode with no interference. Consequently, unlike multi-hop RF systems, no relay selection protocol is required and any relay with

non-full buffer can receive packets from the previous relay and any relay with non-empty buffer can transmit packets to the subsequent relay. We denote by l_n the number of packets present in the buffer of the n-th relay R_n with $0 \leq l_n \leq L$. In this case, the link R_{n-1}-R_n is considered available if this link is not in outage (with probability $1-p_n$) with $l_{n-1} \neq 0$ and $l_n \neq L$. Furthermore, no CSI acquisition is needed where R_{n-1} transmits a packet to R_n and frees this packet from its buffer if it receives an acknowledgement (ACK) from R_n and keeps it in the buffer otherwise (negative-acknowledgement NACK). Finally, S is assumed to have an infinite supply of packets.

C. Markov Chain Analysis

A Markov chain analysis will be adopted for studying the BA system [6]. A state of the Markov chain is represented by the numbers of packets present in the buffers of each of the N_r relays and is denoted by $\mathbf{l} \triangleq (l_1, \ldots, l_{N_r})$ resulting in a total of $(L+1)^{N_r}$ states. The evolution between the states will be captured by the $(L+1)^{N_r} \times (L+1)^{N_r}$ state transition matrix $\mathbf{A}$. In what follows, the function $\mathfrak{N}(\mathbf{l}) = \mathfrak{N}((l_1, \ldots, l_{N_r})) = 1 + \sum_{n=1}^{N_r} l_n (L+1)^{N_r - n}$ will be used to number the states where this function defines a one-to-one relation between the set of all possible states $\{0, \ldots, L\}^{N_r}$ and the set of integers $\{1, \ldots, (L+1)^{N_r}\}$. Denoting by $t_{\mathbf{l},\mathbf{l}'}$ the probability of moving from state $\mathbf{l}$ to state $\mathbf{l}'$, the $(\mathfrak{N}(\mathbf{l}'), \mathfrak{N}(\mathbf{l}))$-th element of the matrix $\mathbf{A}$ is equal to $t_{\mathbf{l},\mathbf{l}'}$.

The steady-state distribution of the states is captured by the $(L+1)^{N_r} \times 1$ dimensional vector π. For $\mathbf{l} = (l_1, \ldots, l_{N_r})$, the $\mathfrak{N}(\mathbf{l})$-th element of π will be denoted by $\pi_{(l_1,\ldots,l_{N_r})}$ which stands for the steady-state probability of having l_n packets in the n-th buffer for $n = 1, \ldots, N_r$. The steady-state distribution can be obtained by solving the equation $\mathbf{A}\pi = \pi$ under the condition that elements of π add up to one: $\sum_{n=1}^{N_r} \sum_{l_n=0}^{L} \pi_{(l_1,\ldots,l_{N_r})} = 1$ [6].

III. Performance Analysis with One Relay

A. State Transition Matrix and Steady-State Distribution

In the case of one relay, the N_r-dimensional state vector $\mathbf{l}$ will reduce to a scalar $\mathbf{l} = l_1$ that will be denoted by $\mathbf{l} \triangleq l$. In this case, $\mathfrak{N}(l) = l+1$ implying that π_l will correspond to the $(l+1)$-th element of π. Finally, the single relay R_1 will be denoted by R for simplicity.

For $l = 0$, no packets can be transmitted along R-D. Therefore, transitions to the states $l' = l$ and $l' = l+1$ are possible with $t_{0,0} = p_1$ and $t_{0,1} = 1-p_1$ where the buffer will remain empty if the S-R link is in outage while the buffer will have one packet if this link is not in outage.

When $l = L$, transitions to the states $l' = l$ and $l' = l-1$ are possible with $t_{L,L} = p_2$ and $t_{L,L-1} = 1-p_2$. In fact, in this case, no packets can be received from S implying that the buffer size will remain the same if the R-D link is in outage and it will decrease by 1 otherwise.

If $l \neq 0$ and $l \neq L$, transitions to the states $l' = l-1$, $l' = l$ and $l' = l+1$ are possible with:

$$\begin{aligned} &t_{l,l-1} = p_1(1-p_2) \quad ; \quad t_{l,l+1} = p_2(1-p_1) \\ &t_{l,l} = p_1p_2 + (1-p_1)(1-p_2) \quad , \quad l = 1, \ldots, L-1, \end{aligned} \tag{5}$$

where, in this case, the relay is neither full nor empty. The buffer size will decrease by 1 if the S-R link is in outage while the R-D link is not in outage and it will increase by 1 if the S-R link is not in outage while the R-D link is in outage. The buffer will keep the same size either if both S-R and R-D links are in outage (i.e. no packet is received and no packet is transmitted) or if both links are not in outage (i.e. one packet received while another packet is transmitted).

Proposition *1:* The steady-state probability vector $\pi = [\pi_0 \cdots \pi_L]^T$ is given by:

$$\begin{cases} \pi_0 = \frac{p_2(r-1)}{(r^L-1)+(r-1)(p_2+p_1r^L-1)}, \\ \pi_l = \frac{r^l}{p_2}\pi_0 \quad ; \quad l = 1, \ldots, L-1, \\ \pi_L = \frac{p_1 r^L}{p_2}\pi_0, \end{cases} \quad ; \quad r \triangleq \frac{p_2(1-p_1)}{p_1(1-p_2)}. \tag{6}$$

Proof: The proof is provided in Appendix A. ∎

When R is closer to S, $p_1 < p_2$ ($r > 1$) and it can be proven that $\max_{l=0,\ldots,L}\{\pi_l\} = \pi_{L-1}$ implying that the buffer has $L-1$ packets most of the time at steady-state. Similarly, when R is closer to D, $p_1 > p_2$ ($r < 1$) and $\max_{l=0,\ldots,L}\{\pi_l\} = \pi_1$ implying that the buffer has one packet most of the time. In fact, in the first (resp. second) case, the better quality of the S-R (resp. R-D) link will privilege filling (resp. emptying) the buffer at a faster pace.

B. Outage Probability (OP) and Average Packet Delay (APD)

1) Outage Probability: Consistently with the definition adopted in [6]–[11] and many of the references therein, a system outage event occurs when no change in the status of any buffer is observed meaning that the system is not capable of successfully transferring packets between any pair of adjacent nodes. This outage of the system is clearly caused by the unavailability of all of its constituent links, which in turn prevents the relays and/or the destination from successfully receiving packets. When the buffer is empty, it will remain in this state when the S-R link is in outage (with probability p_1) since no packets can be transmitted along the R-D link when the buffer is empty. Similarly, a full buffer will remain full when the R-D link is in outage (with probability p_2) since a full buffer can not accept any packets from S. In the case where the buffer is neither full nor empty, an outage event will occur when both hops are in outage with probability p_1p_2. Therefore, the system outage probability can be calculated as follows:

$$P_{\text{out}} = p_1\pi_0 + \sum_{l=1}^{L-1}[p_1p_2\pi_l] + p_2\pi_L, \tag{7}$$

that, from (6), simplifies to $P_{\text{out}} = \pi_0\left[p_1 + p_1\sum_{l=1}^{L-1} r^l + p_1r^L\right]$ resulting in $P_{\text{out}} = p_1\pi_0\frac{r^{L+1}-1}{r-1}$ using the geometric series sum formula. Replacing π_0 by its value from (6) results in:

$$P_{\text{out}} = p_1p_2\frac{r^{L+1}-1}{(r^L-1)+(r-1)(p_2+p_1r^L-1)}. \tag{8}$$

It can be proven that (8) is invariant under the transformation $(p_1, p_2) \rightarrow (p_2, p_1)$ implying that the OP remains unchanged if the lengths of the two hops are interchanged.

2) Average Packet Delay: The buffering of the packets at R will induce a delay in the delivery of these packets to D. Following from Little's law [26] and from the analysis presented in [21]:

$$APD = \frac{\bar{L}+1}{\eta} - 1, \tag{9}$$

where $\bar{L}$ stands for the average queue length while η stands for the input throughput at R. In fact, APD can be written as $APD = APD_{\rm S} + APD_{\rm R}$ where $APD_{\rm S}$ and $APD_{\rm R}$ stand for the average delays at S and R, respectively. Now, it was proven in [21] that $APD_{\rm S} = \frac{1-\eta}{\eta}$ while $APD_{\rm R} = \frac{\bar{L}}{\eta}$ following from Little's law [26]. Combining the above relations results in (9).

The average queue length is given by $\bar{L} = \sum_{l=0}^{L} l\pi_l = \left[\sum_{l=1}^{L-1} lr^l + p_1 L r^L\right] \frac{\pi_0}{p_2}$ from (6). After straightforward evaluation, the last expression simplifies to:

$$\bar{L} = \frac{\pi_0}{p_2}\frac{r}{(r-1)^2}\left[\left(L-1+\frac{Lp_1}{r}(r-1)^2\right)r^L - Lr^{L-1} + 1\right]. \tag{10}$$

When the buffer is full, no packets can be transmitted along S-R implying a zero input throughput at R. Otherwise, when the buffer is not full, a packet is successfully delivered to R only when S-R is not in outage. Consequently, $\eta = (1-p_1)(1-\pi_L)$ which, from (6), results in:

$$\eta = (1-p_1)\left[1 - \frac{p_1(r-1)r^L}{(r^L-1)+(r-1)(p_2+p_1r^L-1)}\right]. \tag{11}$$

3) Special cases $d_1 = d_2$ and $L = 1$: The expressions derived in (6), (8) and (10)-(11) can be further simplified into more tractable expressions in the special cases $d_1 = d_2$ and $L = 1$.

The case $d_1 = d_2$ implies that $p_1 = p_2$ and $r = 1$. Consequently, (6) simplifies to:

$$\pi_0 = \pi_L = \frac{p_1}{2p_1+L-1} \;;\; \pi_1 = \cdots = \pi_{L-1} = \frac{1}{2p_1+L-1}, \tag{12}$$

implying that (8) and (10)-(11) will simplify to:

$$P_{\rm out} = p_1^2\frac{L+1}{2p_1+L-1} \;;\; \bar{L} = \frac{L}{2} \;;\; \eta = \frac{(1-p_1)(p_1+L-1)}{2p_1+L-1}. \tag{13}$$

If $L = 1$, (6) simplifies to $\pi_0 = \frac{1-p_2}{2-p_1-p_2}$ and $\pi_1 = \frac{1-p_1}{2-p_1-p_2}$ resulting in:

$$P_{\rm out} = \frac{p_1+p_2-2p_1p_2}{2-p_1-p_2} \;\;;\;\; \bar{L} = \frac{1-p_1}{2-p_1-p_2} \;\;;\;\; \eta = \frac{(1-p_1)(1-p_2)}{2-p_1-p_2}. \tag{14}$$

C. Asymptotic Analysis

We next provide an asymptotic analysis that holds for $P_M \gg 1$ ($p_1 \ll 1$ and $p_2 \ll 1$).

1) $L = 1$: Equation (14) shows that $P_{\rm out} \to \frac{p_1+p_2}{2}$. This OP is comparable to that achieved by buffer-free ($L = 0$) two-hop systems: $P_{\rm out} = 1-(1-p_1)(1-p_2) = p_1+p_2-p_1p_2 \to p_1+p_2$ [4]. This implies that, when R is equipped with a buffer of size one, the OP is reduced by a factor of $1/2$ without any improvement in the diversity order with respect to buffer-free systems. In fact, $P_{\rm out}$ can be further approximated by $\frac{1}{2}\max\{p_1,p_2\}$ and $\max\{p_1,p_2\}$ for $L = 1$ and $L = 0$, respectively. This implies that, in both cases, the diversity order is $\min\{\beta_1,\beta_2\}$ following from (3)-(4). On the other hand, (14) implies that $\bar{L} \to \frac{1}{2}$ and $\eta \to \frac{1}{2}$ resulting in $APD = 2$ from (9). From the above analysis, we conclude that buffers with capacity exceeding one packet must be used; otherwise, a delay of two packet durations will be induced without any diversity gain.

2) $L \geq 2$: In the case $d_1 = d_2$, the values in (13) tend to the following asymptotic expressions:

$$P_{\rm out} \to \frac{L+1}{L-1}p_1^2 = \left(\left[\frac{L-1}{L+1}\right]^{1/2\beta}\frac{G_1P_M}{2a_1^{1/\beta}}\right)^{-2\beta} \;\;;\;\; \bar{L} = \frac{L}{2} \;\;;\;\; \eta \to 1 \;\;;\;\; APD \to \frac{L}{2}, \tag{15}$$

where $\beta = \beta_1 = \beta_2$, $a_1 = a_2$ and $G_1 = G_2$ in this case.

Equation (15) shows that any buffer size $L \geq 2$ is capable of achieving a diversity order of 2β that is double that achieved by buffer-free systems. Moreover, the OP decreases with L while $APD \to \frac{L}{2}$ increases with L implying that a compromise must be made on the choice of L.

We assume that $d_1 \neq d_2$ in what follows. For $p_1 \ll 1$ and $p_2 \ll 1$, $1-p_1 \approx 1$ and $1-p_2 \approx 1$ implying that $r = \frac{p_2(1-p_1)}{p_1(1-p_2)} \to \frac{p_2}{p_1}$. The denominator of the probability π_0 in (6) can be written as $(1-p_1+p_1r)r^L - (1-p_2)r - p_2 \to (1-p_1+p_2)r^L - r \to r^L - r$. Therefore:

$$\pi_0 \to p_2\frac{\frac{p_2}{p_1}-1}{\left(\frac{p_2}{p_1}\right)^L - \frac{p_2}{p_1}}. \tag{16}$$

Similarly, the OP in (8) will tend to the following asymptotic value:

$$P_{\rm out} \to \frac{p_2^{L+1}-p_1^{L+1}}{p_2^{L-1}-p_1^{L-1}} \to \left[\max\{p_1,p_2\}\right]^2, \tag{17}$$

since, if $p_2 > p_1$ (resp. $p_2 < p_1$), then $P_{\rm out} \to \frac{p_2^{L+1}}{p_2^{L-1}} = p_2^2$ (resp. $P_{\rm out} \to \frac{-p_1^{L+1}}{-p_1^{L-1}} = p_1^2$).

Following from (3)-(4), equation (17) shows that the diversity order achieved by buffer-aided two-hop systems is $2\beta = 2\min\{\beta_1,\beta_2\}$ (for all values of $L \geq 2$) thus highlighting a two-fold increase in the diversity order with respect to buffer-free systems. Equation (17) also reveals the important observation that the asymptotic OP does not depend on L in the case $d_1 \neq d_2$.

While the asymptotic OP is the same for $p_2 > p_1$ and $p_2 < p_1$, the APD will vary between these two cases. When R is closer to S, $r = \frac{p_2}{p_1} > 1$ implying, from (16), that $\pi_0 \to p_2\frac{1}{(p_2/p_1)^{L-1}}$. From (6), $\pi_{L-1} \to \frac{1}{p_2}\left(\frac{p_2}{p_1}\right)^{L-1}\pi_0 \to 1$ implying that at equilibrium the buffer is in the state $l = L-1$ all of the time. In this case, $\bar{L} = \sum_{l=0}^{L} l\pi_l \to L-1$. Moreover, $\eta = (1-p_1)(1-\pi_L) = (1-p_1)(1-p_1r\pi_{L-1}) \to (1-p_1)(1-p_2)$ as $\pi_{L-1} \to 1$. Therefore, from (9):

$$APD \to \frac{L}{(1-p_1)(1-p_2)} - 1 \to L-1. \tag{18}$$

Similarly, when R is closer to D, $p_2 < p_1$ and $r = \frac{p_2}{p_1} < 1$ implying that the probability in (16) will tend to $\pi_0 \to p_2 \frac{-1}{-p_2/p_1} = p_1$. From (6), $\pi_1 = \frac{r}{p_2}\pi_0 = \frac{1}{p_1}\pi_0 \to 1$ implying that at equilibrium the buffer is in the state $l = 1$ all of the time. In this case, $\bar{L} = \sum_{l=0}^{L} l\pi_l \to 1$. Moreover, $\eta = (1-p_1)(1-\pi_L) = (1-p_1)(1-\frac{p_1}{p_2}r^L\pi_0) \to (1-p_1)\left(1-p_1\left(\frac{p_2}{p_1}\right)^{L-1}\right) \to (1-p_1)$. Therefore, from (9):

$$APD \to \frac{2}{1-p_1} - 1 \to 1. \tag{19}$$

D. Analyzing the Results and Implications on the System Design

Consider the two symmetrical locations (with respect to the midpoint of [S D]) (d_1, d_2) and (d_2, d_1) with $d_1 < d_2$. The following observations pertaining to the network design can be made:

- The choice $L = 1$ must be omitted since it does not result in any diversity advantage.
- The OP is the same for both locations. The APD increases as $L-1$ in the first location while it is constant (and equal to 1) in the second location. Therefore, it is better to place R in the second location since the OP is the same while the APD is smaller.
- However, from (17), the OP does not depend on L for $L \geq 2$; therefore, there is no reason for increasing L beyond 2. Now, for $L=2$, $L-1=1$ and the two locations will yield not only the same OP but also the same APD.

Now, comparing the scenarios $d_1 = d_2$ and $d_1 \neq d_2$, the following conclusions can be drawn:

- The first scenario results in a smaller OP since $\max\{p_1, p_2\}$ is minimized for $p_1 = p_2$. However, this choice is associated with a delay that increases as $\frac{L}{2}$.
- As highlighted before, $L=2$ constitutes the best choice in the second scenario. This scenario is characterized by a smaller APD (of 1) and a higher OP compared to scenario 1.

IV. Asymptotic Analysis with any Number of Relays

A. General Comments

It is important to highlight that the theoretical condition $d_1 = d_2$, that was treated separately in the case of one relay, is almost impossible to realize in realistic networks. In fact, d_1 and d_2 are in the order of few kilometers and shifting the relay's location by a fraction of a meter while deploying the network will favor lower outages along one of the two hops compared to the other hop. Even though the outage probabilities along the different hops can be made approximately the same by an appropriate statistical power allocation strategy, however, this approach involves a ceratin level of CSI acquisition that adds to the complexity of the system. In all circumstances, making these probabilities identical is not appealing from a delay point of view as has been highlighted in Section III-D in the context of one relay. Finally, we also exclude the case $L = 1$ from our analysis since this buffer size fails in capturing any diversity advantage. Next, we focus on the asymptotic case $P_M \gg 1$ resulting in $p_n \ll 1$ for $n = 1, \ldots, N_r + 1$. We recall from (3) that the index of the worst (bottleneck) hop is denoted by $\tilde{n}$ where $p_{\tilde{n}} = \max\{p_1, \ldots, p_{N_r+1}\}$.

The asymptotic analysis revolves around the identification of a closed-subset of states $\mathcal{S}$ where, at steady-state, the system is in the states of $\mathcal{S}$ with a probability tending to 1. From [27, Sec. 9.5], the set $\mathcal{S}$ is said to be closed if no state in $\mathcal{S}$ leads to any state outside $\mathcal{S}$. In other words, $\mathcal{S}$ defines a closed-subset if $t_{\mathbf{l},\mathbf{l}'} = 0 \; \forall \, \mathbf{l} \in \mathcal{S}$ and $\mathbf{l}' \notin \mathcal{S}$. The identification of the closed-subset is very useful since it dramatically simplifies the analysis because the states in the closed-subset are recurrent [27, Sec. 9.4]. In other words, only the states in the closed-subset $\mathcal{S}$ can be considered for the OP and APD calculations since the number of time slots in which the system is in one of the transient states outside $\mathcal{S}$ tends to zero. In fact, after a certain number of transitions among the transient states in $\bar{\mathcal{S}}$, the Markov chain will eventually move to a certain state in $\mathcal{S}$ and remain in this closed-subset since the transition probabilities out of this subset tend to zero.

Following from the above observations, the asymptotic OP can be derived from:

$$P_{\text{out}} \to \sum_{\mathbf{l}=(l_1,\ldots,l_{N_r})\in\mathcal{S}} \pi_{\mathbf{l}} \mathrm{P}_{\mathbf{l}}, \tag{20}$$

where $P_{\mathbf{l}}$ stands for the probability of outage when the system is in the state $\mathbf{l}$:

$$\mathrm{P}_{\mathbf{l}} = \prod_{n=1}^{N_r+1} \mathfrak{p}_n \;\; ; \;\; \mathfrak{p}_n = \begin{cases} 1, & l_{n-1} = 0 \;\text{ or }\; l_n = L; \\ p_n, & \text{otherwise.} \end{cases}, \tag{21}$$

where $\mathfrak{p}_n$ stands for the unavailability probability with which no packet can be communicated along the n-th hop R_{n-1}-R_n. This probability captures both the channel condition and unavailability of the n-th hop following from the buffers' states. In fact, if the buffer at R_{n-1} is empty or the buffer at R_n is full then no packet can be transmitted along the n-th hop resulting in $\mathfrak{p}_n = 1$ (unavailable link). Otherwise, a packet can not be delivered only if the n-hop is in outage with probability p_n. Finally, for the first (resp. last) hop, there is no need to check for the condition $l_{n-1} = 0$ (resp. $l_n = L$) since l_n is defined for $n = 1, \ldots, N_r$ (i.e. $n \neq 0$ and $n \neq N_r + 1$).

Following from Little' law [26], the APD can be calculated from:

$$APD = \sum_{n=1}^{N_r} \frac{\bar{L}_n}{\eta_n} + \frac{1}{\eta_1} - 1, \tag{22}$$

where $\bar{L}_n$ and η_n stand for the average queue length and input throughput at R_n, respectively. In (22), the term $\frac{1}{\eta_1} - 1$ stands for the average delay at S [6], [21] (where η_1 was denoted by η in (9) and (11) in the case of one relay). A packet is successfully delivered to R_n if the buffer at R_n is not full, the buffer at R_{n-1} is not empty and the n-th hop is not in outage resulting in:

$$\eta_n = (1-p_n)\left(1-\pi_L^{(n)}\right)\left(1-\pi_0^{(n-1)}\right) \;\; ; \;\; n = 1, \ldots, N_r, \tag{23}$$

where $\pi_l^{(n)}$ stands for the steady-state probability of having l packets in the buffer of R_n that can be calculated from $\pi_l^{(n)} = \sum_{l_1=0}^{L}\cdots\sum_{l_{n-1}=0}^{L}\sum_{l_{n+1}=0}^{L}\cdots\sum_{l_{N_r}=0}^{L}\pi_{(l_1,\ldots,l_{n-1},l,l_{n+1},\ldots,l_{N_r})}$. We assume that $\pi_0^{(0)} = 0$ in (23) since S always has packets to transmit.

In this section, we will prove that $\pi_0^{(n)} \to 0$ and $\pi_L^{(n)} \to 0$ for $n = 1, \ldots, N_r$ implying that $\eta_n \to 1 - p_n \to 1$. Therefore, (22) will tend to the following asymptotic expression:

$$APD = \sum_{n=1}^{N_r} \bar{L}_n. \tag{24}$$

In order to offer more insights on the calculation methodology, we first present the asymptotic analysis in the special case $N_r = 2$ and then we carry out the extension to the general case.

B. $N_r = 2$

1) State Transition Matrix: The following cases arise when evaluating the probabilities $t_{\mathbf{l},\mathbf{l}'}$.

Case 1: $\mathbf{l} = (0,0)$. Since both buffers are empty, then no transmissions can occur along the second and third hops in this case. Now, if the first hop is in outage, then the first buffer will remain empty resulting in $t_{(0,0),(0,0)} = p_1$. On the other hand, if the first hop is not in outage, then the number of packets in the first buffer will increase by one resulting in $t_{(0,0),(1,0)} = 1 - p_1$.

Case 2: $\mathbf{l} = (L,0)$. In this case, no transmissions can occur along the first hop since the first buffer is full while no transmissions can occur along the third hop since the second buffer is empty. Now, the system will remain in the same state $\mathbf{l}' = (L,0)$ if the second hop is in outage and it will move to the state $\mathbf{l}' = (L-1,1)$ if the second hop is not in outage. Consequently, $t_{(L,0),(L,0)} = p_2$ and $t_{(L,0),(L-1,1)} = 1 - p_2$.

Case 3: $\mathbf{l} = (L,L)$ implying that no transmissions can take place along the first and second hops. Similar to case-1 and case-2, $t_{(L,L),(L,L)} = p_3$ and $t_{(L,L),(L,L-1)} = 1 - p_3$.

Case 4: $\mathbf{l} = (l_1,0)$ where $l_1 = 1, \ldots, L-1$. In this case, no transmissions can occur along the third hop. Consider now the first two hops. When both hops are in outage, the occupancies of both buffer will remain unchanged and $t_{(l_1,0),(l_1,0)} = p_1p_2$. When both hops are not in outage, the occupancy of the first buffer will remain the same (since one packet is received from S and one packet is transmitted to R_2) while the number of packets in the second buffer will increase by one since R_2 will successfully receive a packet from R_1 while no packet is transmitted to D. Consequently, in this case, $t_{(l_1,0),(l_1,1)} = (1-p_1)(1-p_2)$. Similarly, $t_{(l_1,0),(l_1+1,0)} = (1-p_1)p_2$ (resp. $t_{(l_1,0),(l_1-1,1)} = p_1(1-p_2)$) where a successful transmission takes place exclusively along the first (resp. second) hop.

Case 5: $\mathbf{l} = (L,l_2)$ where $l_2 = 1, \ldots, L-1$. In this case, no transmissions can occur along the first hop since the first buffer is full. Similar to case-4, $t_{(L,l_2),(L,l_2)} = p_2p_3$, $t_{(L,l_2),(L-1,l_2)} = (1-p_2)(1-p_3)$, $t_{(L,l_2),(L,l_2-1)} = p_2(1-p_3)$ and $t_{(L,l_2),(L-1,l_2+1)} = (1-p_2)p_3$.

Case 6: $\mathbf{l} = (0,l_2)$ where $l_2 = 1, \ldots, L$ or $\mathbf{l} = (l_1,L)$ where $l_1 = 1, \ldots, L-1$. In this case, no transmissions can occur along the second hop since either the first buffer is empty or/and the second buffer is full. Consequently, the occupancy of the first buffer will increase by one if the first hop is not in outage; otherwise, it will remain the same. Similarly, the occupancy of the second buffer will decrease by one if the third hop is not in outage; otherwise, it will remain the same. Consequently, $t_{\mathbf{l},\mathbf{l}} = p_1p_3$, $t_{\mathbf{l},\mathbf{l}+(1,0)} = (1-p_1)p_3$, $t_{\mathbf{l},\mathbf{l}+(0,-1)} = p_1(1-p_3)$ and $t_{\mathbf{l},\mathbf{l}+(1,-1)} = (1-p_1)(1-p_3)$.

Case 7: $\mathbf{l} = (l_1,l_2)$ where $l_1 = 1, \ldots, L-1$ and $l_2 = 1, \ldots, L-1$. In this case, none of the buffers is full or empty and transmissions can take place along all hops. Consequently:

$$\begin{aligned}
&t_{\mathbf{l},\mathbf{l}} = p_1p_2p_3 + (1-p_1)(1-p_2)(1-p_3)\ ;\\
&t_{\mathbf{l},\mathbf{l}+(-1,0)} = p_1(1-p_2)(1-p_3)\ ;\\
&t_{\mathbf{l},\mathbf{l}+(1,-1)} = (1-p_1)p_2(1-p_3)\ ;\\
&t_{\mathbf{l},\mathbf{l}+(0,1)} = (1-p_1)(1-p_2)p_3\ ;\\
&t_{\mathbf{l},\mathbf{l}+(1,0)} = (1-p_1)p_2p_3\ ;\\
&t_{\mathbf{l},\mathbf{l}+(-1,1)} = p_1(1-p_2)p_3\ ;\\
&t_{\mathbf{l},\mathbf{l}+(0,-1)} = p_1p_2(1-p_3),
\end{aligned} \tag{25}$$

where, generally speaking, (i): the buffer size will increase by one if the previous hop is not in outage while the subsequent hop is in outage, (ii): the buffer size will decrease by one if the previous hop is in outage while the subsequent hop is not in outage and (iii): the buffer size will remain the same if the previous and subsequent hops have the same status. It is worth noting that in case-7, $2^{N_r+1} - 1 = 7$ transitions are possible where the scenarios when all hops are or are not in outage will keep the system in the same state with probability $t_{\mathbf{l},\mathbf{l}}$.

2) Asymptotic Steady-State Distribution:

Proposition *2:* For asymptotically large values of P_M, the closed-subset $\mathcal{S}$ is given by:

$$\mathcal{S} = \begin{cases} \{(0,0),(0,1),(1,0),(1,1)\}, & \tilde{n} = 1;\\ \{(L,0),(L-1,1)\}, & \tilde{n} = 2;\\ \{(L,L),(L-1,L),(L,L-1),(L-1,L-1)\}, & \tilde{n} = 3. \end{cases} \tag{26}$$

Proof: The proof is provided in Appendix B. ■

Following from the asymptotic transition probabilities derived in Appendix B, the transitions between the states of the closed-subset are depicted in Fig. 2. Capturing the steady-state distribution of the recurrent states (inside $\mathcal{S}$) by the vector π', elements of π' will add up to 1 asymptotically for the reasons stated in Section IV-A. The steady-state distribution of the recurrent states can be obtained by solving $\mathbf{A}_{\text{red}}^{(\tilde{n})}\pi' = \pi'$ (with the elements of π' adding up to 1) where $\pi' = [\pi_{(0,0)}, \pi_{(0,1)}, \pi_{(1,0)}, \pi_{(1,1)}]^T$, $\pi' = [\pi_{(L,0)}, \pi_{(L-1,1)}]^T$ and $\pi' = [\pi_{(L,L)}, \pi_{(L-1,L)}, \pi_{(L,L-1)}, \pi_{(L-1,L-1)}]^T$ for $\tilde{n} = 1$, $\tilde{n} = 2$ and $\tilde{n} = 3$, respectively.

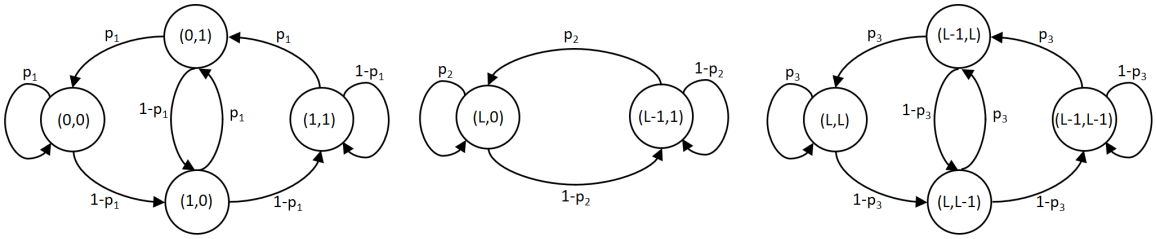

Fig. 2. The closed-subsets and the corresponding transitions in the case of two relays.

The reduced state transition matrices are given by:

$$\mathbf{A}_{\text{red}}^{(2)} = \begin{bmatrix} p_2 & p_2 \\ 1-p_2 & 1-p_2 \end{bmatrix} \; ;$$
$$\mathbf{A}_{\text{red}}^{(\tilde{n})} = \begin{bmatrix} p_{\tilde{n}} & p_{\tilde{n}} & 0 & 0 \\ 0 & 0 & p_{\tilde{n}} & p_{\tilde{n}} \\ 1-p_{\tilde{n}} & 1-p_{\tilde{n}} & 0 & 0 \\ 0 & 0 & 1-p_{\tilde{n}} & 1-p_{\tilde{n}} \end{bmatrix} \; ; \; \tilde{n}=1,3, \tag{27}$$

As a conclusion, the identification of the closed-subset (that is possible only for asymptotic values of P_M) simplifies the solution for the steady-state distribution. In fact, instead of solving $\mathbf{A}\pi = \pi$ to find the $(L+1)^2$ elements of π, we solve the simpler equation $\mathbf{A}_{\text{red}}^{(\tilde{n})}\pi' = \pi'$ involving 4, 2 and 4 unknowns for $\tilde{n}=1$, $\tilde{n}=2$ and $\tilde{n}=3$, respectively. In Appendix C, we prove that:

$$\pi' = \begin{cases} \left[\pi_{(0,0)}, \pi_{(0,1)}, \pi_{(1,0)}, \pi_{(1,1)}\right]^T, & \tilde{n}=1; \\ \left[\pi_{(L,0)}, \pi_{(L-1,1)}\right]^T, & \tilde{n}=2; \\ \left[\pi_{(L,L)}, \pi_{(L-1,L)}, \pi_{(L,L-1)}, \pi_{(L-1,L-1)}\right]^T, & \tilde{n}=3. \end{cases}.$$
$$= \begin{cases} \left[p_1^2, p_1(1-p_1), p_1(1-p_1), (1-p_1)^2\right]^T, & \tilde{n}=1; \\ \left[p_2, 1-p_2\right]^T, & \tilde{n}=2; \\ \left[p_3^2, p_3(1-p_3), p_3(1-p_3), (1-p_3)^2\right]^T, & \tilde{n}=3. \end{cases}. \tag{28}$$

3) Asymptotic OP and APD: For $\tilde{n}=1$, $\mathrm{P}_{(0,0)} = p_1$, $\mathrm{P}_{(0,1)} = p_1p_3$, $\mathrm{P}_{(1,0)} = p_1p_2$ and $\mathrm{P}_{(1,1)} = p_1p_2p_3$ following from (21). Replacing these values as well as (28) in (20) results in $P_{\text{out}} = p_1^3 + p_1^2p_3(1-p_1) + p_1^2p_2(1-p_1) + p_1p_2p_3(1-p_1)^2 \rightarrow p_1^3 + p_1^2p_3 + p_1^2p_2 + p_1p_2p_3$ that tends to p_1^3 since $\max\{p_1,p_2,p_3\} = p_1$ in this case. Similarly, for $\tilde{n}=2$, $\mathrm{P}_{(L,0)} = p_2$ and $\mathrm{P}_{(L-1,1)} = p_1p_2p_3$ which from (20) and (28) results in $P_{\text{out}} = p_2^2 + p_1p_2p_3(1-p_2) \rightarrow p_2^2$. Finally, for $\tilde{n}=3$, $\mathrm{P}_{(L,L)} = p_3$, $\mathrm{P}_{(L-1,L)} = p_1p_3$, $\mathrm{P}_{(L,L-1)} = p_2p_3$ and $\mathrm{P}_{(L-1,L-1)} = p_1p_2p_3$ resulting in $P_{\text{out}} = p_3^3 + p_1p_3^2(1-p_3) + p_2p_3^2(1-p_3) + p_1p_2p_3(1-p_3)^2 \rightarrow p_3^3$ since $\max\{p_1,p_2,p_3\} = p_3$ in this case. As a conclusion:

$$P_{\text{out}} \rightarrow \begin{cases} \left[\max\{p_1,p_2,p_3\}\right]^3, & \tilde{n}=1 \;\text{ or }\; \tilde{n}=3; \\ \left[\max\{p_1,p_2,p_3\}\right]^2, & \tilde{n}=2. \end{cases}, \tag{29}$$

implying, from (3)-(4), a three-fold increase in the diversity order only if the bottleneck hop corresponds to the first hop or last hop.

The interpretation of (29) is as follows. For $\tilde{n}=1$, the outage of the bottleneck link S-R_1 over two consecutive time slots (with probability p_1^2) will incur the emptying of the two buffers since, from Fig. 2, it can be observed that it takes at most two transitions to reach the state $(0,0)$ from any other state. Once in the state $(0,0)$, no transmissions can take place along the second and third hops implying that an additional outage event along the first hop (with probability p_1) will result in a system outage. The same interpretation holds for the case $\tilde{n}=3$ where the state (L,L) can be reached in two transitions at most implying that two successive outages of hop-3 (with probability p_3^2) will result in filling both buffers. Now, an additional outage of hop-3 in a third slot will result in a system outage with probability p_3^3. For $\tilde{n}=2$, a single outage of the bottleneck link hop-2 (with probability p_2) will bring the system to the state $(L,0)$ from Fig. 2. Now, the first buffer is full and the second buffer is empty implying that no transmissions can take place along the first and third hops. This implies that an additional outage of hop-2 is sufficient to cause a system outage. This justifies why in this case the OP is p_2^2 (and not p_2^3).

Regarding the APD, for $\tilde{n}=1$, (28) shows that $\pi_{(1,1)} = 1-p_1 \rightarrow 1$ implying that each one of the buffers contains one packet most of the time at steady-state. Consequently, the probability of having either empty or full buffers tends to zero and $\eta_n \rightarrow 1$ in (23) for $n=1,2$. In this case, $\bar{L}_1 \rightarrow 1$ and $\bar{L}_2 \rightarrow 1$ resulting in $APD \rightarrow 2$ from (24). The same holds for the other values of $\tilde{n}$ where the results are summarized as follows following from (24) and (28):

$$\begin{cases} \pi_{(1,1)} \rightarrow 1 \Rightarrow \bar{L}_1 \rightarrow 1 \;,\; \bar{L}_2 \rightarrow 1 \\ \qquad\qquad \Rightarrow APD \rightarrow 2, & \tilde{n}=1; \\ \pi_{(L-1,1)} \rightarrow 1 \Rightarrow \bar{L}_1 \rightarrow L-1 \;,\; \bar{L}_2 \rightarrow 1 \\ \qquad\qquad \Rightarrow APD \rightarrow L, & \tilde{n}=2; \\ \pi_{(L-1,L-1)} \rightarrow 1 \Rightarrow \bar{L}_1 \rightarrow L-1 \;,\; \bar{L}_2 \rightarrow L-1 \\ \qquad\qquad \Rightarrow APD \rightarrow 2(L-1), & \tilde{n}=3; \end{cases}. \tag{30}$$

The interpretation of (30) is as follows. When the first hop is the bottleneck link, the relatively inferior quality of this hop will reduce the input throughput at R_1 thus thinning out the occupancy not only of the buffer at R_1 but also of the buffer at R_2 since the flow of packets along $\mathrm{R}_1 \rightarrow \mathrm{R}_2 \rightarrow \mathrm{D}$ is almost guaranteed given the relatively lower outage probabilities along the last two hops. These buffers tend to have one packet each without being fully depleted since even the bottleneck link is assumed to have a low outage probability ($p_1 \ll 1$) in the asymptotic regime. Now, when the third hop is the bottleneck link, the output throughput from R_2 is minimal

$$\begin{cases} (l_{\tilde{n}-1}, l_{\tilde{n}}), (l_{\tilde{n}-2}, l_{\tilde{n}+1}), \ldots, (l_1, l_{2\tilde{n}-2}) \in \{(L-1,1),(L,0)\}, \\ l_{2\tilde{n}-1}, \ldots, l_{N_r} \in \{0,1\}. \end{cases} ; \quad \xi = \tilde{n}-1; \\ \begin{cases} (l_{\tilde{n}-1}, l_{\tilde{n}}), (l_{\tilde{n}-2}, l_{\tilde{n}+1}), \ldots, (l_{2\tilde{n}-N_r-1}, l_{N_r}) \in \{(L-1,1),(L,0)\}, \\ l_1, \ldots, l_{2\tilde{n}-N_r-2} \in \{L-1, L\}, \end{cases} ; \quad \xi = N_r+1-\tilde{n}. \end{cases} , \tag{33}$$

resulting in the congestion of the two buffers without having them full since $p_3 \ll 1$. Finally, when the second hop is the bottleneck link, the flow of packets along S$\rightarrow$R$_1$ and R$_2$ $\rightarrow$D occurs in a more efficient manner. In this case, the higher outage probability along the bottleneck link will result in filling up the preceding buffer of R$_1$ at a faster pace while the input throughput at R$_2$ will decrease thus reducing the occupancy of its buffer.

4) Conclusions: Define the three sorted distances $d_{(1)} < d_{(2)} < d_{(3)}$ and consider all possible values of the hops' distances (d_1, d_2, d_3). The scenarios $(d_{(1)}, d_{(3)}, d_{(2)})$ and $(d_{(2)}, d_{(3)}, d_{(1)})$ must be avoided since, from (29), these scenarios fail in exploiting the full underlying diversity advantage. The scenarios $(d_{(3)}, d_{(1)}, d_{(2)})$, $(d_{(3)}, d_{(2)}, d_{(1)})$, $(d_{(1)}, d_{(2)}, d_{(3)})$ and $(d_{(2)}, d_{(1)}, d_{(3)})$ are all equivalent in terms of outage behavior. In this context, the advantage of the first two scenarios resides in a smaller APD from (30). However, from (29), it can be observed that the asymptotic OP does not depend on L (for $L \geq 2$) implying that a buffer size of two is sufficient for extracting full diversity. Setting $L = 2$ in (30) implies that $APD \rightarrow 2$ for all values of $\tilde{n}$ showing that the four preceding scenarios will achieve the same OP and APD values in this case.

C. $N_r \geq 2$

1) State Transition Matrix: $2^{N_r+1}-1$ transitions are possible from the state $\mathbf{l} = (l_1, \ldots, l_{N_r})$ where these transitions and their corresponding probabilities can be determined as follows. Denote by $\mathcal{A} \subset \{1, \ldots, N_r+1\}$ the set containing the indices of the links that are available where $\mathcal{A}$ can be selected in 2^{N_r+1} possible ways. The transitions are given by:

$$\mathbf{l} = (l_1, \ldots, l_{N_r}) \;\rightarrow\; \mathbf{l}' = (l_1, \ldots, l_{N_r}) + (\delta_1, \ldots, \delta_{N_r}) \;, \\ \delta_n = \begin{cases} 0, & (n, n+1) \in \mathcal{A}^2 \text{ or } (n, n+1) \in \bar{\mathcal{A}}^2; \\ 1, & (n, n+1) \in \mathcal{A} \times \bar{\mathcal{A}}; \\ -1, & (n, n+1) \in \bar{\mathcal{A}} \times \mathcal{A}. \end{cases} ; \\ n = 1, \ldots, N_r, \tag{31}$$

where $\bar{\mathcal{A}}$ denotes the complement of $\mathcal{A}$. For example, when $(n, n+1) \in \mathcal{A} \times \bar{\mathcal{A}}$, R$_n$ can receive a packet along the n-th hop (that is available) while it cannot transmit a packet along the $(n+1)$-th hop (that is not available) implying that its buffer occupancy will increase by 1. The probability of the transition in (31) can be calculated from:

$$t_{\mathbf{l},\mathbf{l}'} = \\ \begin{cases} \prod_{n \in \bar{\mathcal{A}}} \mathfrak{p}_n \prod_{n' \in \mathcal{A}} (1-\mathfrak{p}_{n'}), & (\delta_1, \ldots, \delta_{N_r}) \neq (0, \ldots, 0); \\ \prod_{n=1}^{N_r+1} \mathfrak{p}_n + \prod_{n=1}^{N_r+1} (1-\mathfrak{p}_n), & (\delta_1, \ldots, \delta_{N_r}) = (0, \ldots, 0). \end{cases} , \tag{32}$$

where the probabilities of unavailability $\{\mathfrak{p}_n\}_{n=1}^{N_r+1}$ are defined in (21). The second case in (32) follows since the self-transition $\mathbf{l} \rightarrow \mathbf{l}$ is possible either when all links are available or when all links are unavailable. Note that for this transition, the cases $\mathcal{A} = \{1, \ldots, N_r+1\}$ and $\mathcal{A} = \phi$ (the empty set) need to be combined together. Each of the remaining $2^{N_r+1}-2$ transitions $\mathbf{l} \rightarrow \mathbf{l}' \neq \mathbf{l}$ can occur in one way (each corresponding to a possible value of $\mathcal{A}$ other than the full or empty sets) according to the first probability in (32).

It is worth noting that, from (21), $1 - \mathfrak{p}_n = 0$ if $l_{n-1} = 0$ or $l_n = L$ implying that the corresponding probability in (32) will be zero. In this case, the corresponding transition in (31) cannot take place and the number $2^{N_r+1}-1$ corresponds to the maximum number of transitions that can occur when all of the N_r buffers are neither full nor empty (for example, refer to case-7 in Section IV-B1 in the case $N_r = 2$). Otherwise, the number of possible transitions will drop where in the extreme cases $\mathbf{l_1} = (0, \ldots, 0)$ and $\mathbf{l_2} = (L, \ldots, L)$, only two transitions are possible $\{\mathbf{l_1} \rightarrow \mathbf{l_1}; \mathbf{l_1} \rightarrow \mathbf{l_1} + (1, 0, \ldots, 0)\}$ and $\{\mathbf{l_2} \rightarrow \mathbf{l_2}; \mathbf{l_2} \rightarrow \mathbf{l_2} + (L, \ldots, L, L-1)\}$ (for example, refer to case-1 and case-3 in Section IV-B1 in the case $N_r = 2$).

2) Asymptotic Steady-State Distribution:

Proposition *3:* For $P_M \gg 1$, the subset $\mathcal{S} = \{(l_1, \ldots, l_{Nr})\}$ shown in (33) at the top of the page is closed with the following asymptotic steady-state distribution:

$$\pi_{\mathbf{l}} = \pi_{(l_1,\ldots,l_{N_r})} = \begin{cases} p_{\tilde{n}}^{\mu_0} (1-p_{\tilde{n}})^{N_r-\mu_0}, & \xi = \tilde{n}-1; \\ p_{\tilde{n}}^{\mu_L} (1-p_{\tilde{n}})^{N_r-\mu_L}, & \xi = N_r+1-\tilde{n}. \end{cases} \tag{34}$$

where $\xi \triangleq \min\{\tilde{n}-1, N_r+1-\tilde{n}\}$ while μ_l stands for the number of components of $(l_1, \ldots, l_{N_r})$ that are equal to l.

Proof: The proof is provided in Appendix D. ■

Equation (33) shows that the asymptotic analysis can be simplified by considering the $2^{N_r-\xi}$ states of $\mathcal{S}$ rather than the entire $(L+1)^{N_r}$ states. For $\tilde{n} = 1$ and $\tilde{n} = N_r+1$, $\xi = 0$, and $\mathcal{S}$ simplifies to $\{0,1\}^{N_r}$ and $\{L-1, L\}^{N_r}$, respectively.

3) Asymptotic OP and APD: From (33), $l_n \in \{L-1, L\}$ for $n < \tilde{n}$ and $l_n \in \{0,1\}$ for $n \geq \tilde{n}$. Consequently, since $l_n = 0 \Rightarrow \mathfrak{p}_{n+1} = 1$ and $l_n = L \Rightarrow \mathfrak{p}_n = 1$, then exactly $(\mu_0 + \mu_L)$ terms in P$_{\mathbf{l}}$ in (21) are equal to 1 (in particular, μ_L terms $\mathfrak{p}_n$ for $n < \tilde{n}$ and μ_0 terms $\mathfrak{p}_n$ for $n \geq \tilde{n}$). Therefore, P$_{\mathbf{l}}$ corresponds to the product of $N_r + 1 - (\mu_0 + \mu_L)$ outage probability terms of the form p_n. Now, since $p_n \leq p_{\tilde{n}}$ for $n = 1, \ldots, N_r+1$, then $\mathrm{P}_{\mathbf{l}} \leq p_{\tilde{n}}^{N_r+1-\mu_0-\mu_L}$. Approximating $1-p_{\tilde{n}}$ by 1 in (34), the probability $\pi_{\mathbf{l}}\mathrm{P}_{\mathbf{l}}$ in (20) can be bounded as follows:

$$\pi_{\mathbf{l}}\mathrm{P}_{\mathbf{l}} \leq \begin{cases} p_{\tilde{n}}^{N_r+1-\mu_L}, & \xi = \tilde{n}-1; \\ p_{\tilde{n}}^{N_r+1-\mu_0}, & \xi = N_r+1-\tilde{n}. \end{cases} . \tag{35}$$

From the first equation in (33), $0 \leq \mu_L \leq \tilde{n}-1$ implying, from (35), that $\max_{\mathbf{l}}\{\pi_{\mathbf{l}}\mathrm{P}_{\mathbf{l}}\} = p_{\tilde{n}}^{N_r+1-(\tilde{n}-1)}$ for $\xi = \tilde{n}-1$. Similarly, from the second equation in (33), $0 \leq \mu_0 \leq N_r +$

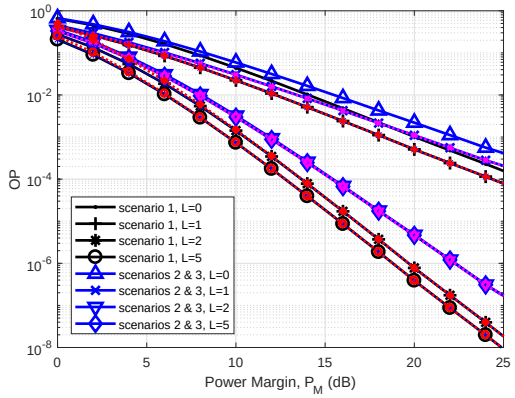

Fig. 3. Outage probability with one relay for $\omega_z/a = 10$. Solid and dotted lines correspond to the exact and asymptotic values, respectively. The asymptotic OP values of $\frac{p_1+p_2}{2}$, (15) and (17) are plotted for scenarios 1-3 ($L = 1$), scenario 1 ($L \geq 2$) and scenarios 2-3 ($L \geq 2$), respectively.

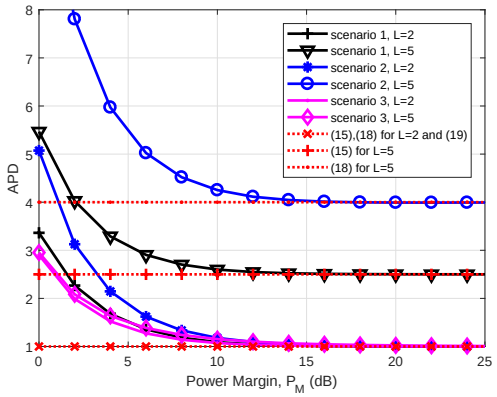

Fig. 4. Average packet delay with one relay for $\omega_z/a = 10$. Solid and dotted lines correspond to the exact and asymptotic values, respectively.

$1-\tilde{n}$ implying that $\max_{\mathbf{l}}\{\pi_{\mathbf{l}}\mathrm{P}_{\mathbf{l}}\} = p_{\tilde{n}}^{N_r+1-(N_r+1-\tilde{n})}$ for $\xi = N_r+1-\tilde{n}$. The above two cases can be combined resulting in the following asymptotic expression of the OP in (20):

$$P_{\text{out}} \to p_{\tilde{n}}^{N_r+1-\xi} = [\max\{p_1,\ldots,p_{N_r+1}\}]^{N_r+1-\min\{\tilde{n}-1,N_r+1-\tilde{n}\}}, \quad (36)$$

implying a $(N_r+1-\xi)$-fold increase in the diversity order compared to buffer-free systems.

Note that $\tilde{n}-1$ (resp. $N_r+1-\tilde{n}$) captures how far the bottleneck hop is from the first (resp. last) hop (in terms of number of hops). The farther the bottleneck hop is from S and D, the larger the value of ξ and the smaller the diversity gain. In this case, the maximum diversity gain is achieved when the first or last hop is the bottleneck hop ($\tilde{n}=1$ or $\tilde{n}=N_r+1$ implying that $\xi=0$) with a diversity gain of N_r+1. The worst cases arise when the central hops constitute the bottleneck ($\tilde{n}=\frac{N_r+2}{2}$ for N_r even and $\tilde{n}\in\{\frac{N_r+1}{2},\frac{N_r+3}{2}\}$ for N_r odd) resulting in the smallest diversity gains of $\frac{N_r}{2}+1$ and $\frac{N_r+1}{2}+1$ for even and odd values of $\tilde{n}$, respectively.

From (34), the state having the highest probability can be obtained by setting $\mu_0=0$ for $\xi=\tilde{n}-1$ and $\mu_L=0$ for $\xi=N_r+1-\tilde{n}$. This maximum probability is equal to $(1-p_{\tilde{n}})^{N_r}\to 1$ for $P_M \gg 1$. From the first equation in (33), the condition $\mu_0=0$ implies that $l_n=L-1$ for $n<\tilde{n}$ and $l_n=1$ for $n\geq\tilde{n}$. The same implication follows from the second equation in (33) for the condition $\mu_L=0$ with $\xi=N_r+1-\tilde{n}$. Therefore, for all values of $\tilde{n}$, the system is in the state $(l_1,\ldots,l_{\tilde{n}-1},l_{\tilde{n}},\ldots,l_{N_r})=(L-1,\ldots,L-1,1,\ldots,1)$ with a steady-state probability tending to 1 for large values of P_M. In other words, $\bar{L}_n\to L-1$ for $n<\tilde{n}$ while $\bar{L}_n\to 1$ for $n\geq\tilde{n}$ implying, from (24), that:

$$APD \to (\tilde{n}-1)(L-1)+(N_r+1-\tilde{n}) = N_r+(L-2)(\tilde{n}-1), \quad (37)$$

implying that the asymptotic APD increases linearly with N_r and linearly with L for $\tilde{n}\neq 1$. The case $\tilde{n}=1$ results in the minimum APD of N_r while the case $\tilde{n}=N_r+1$ results in the maximum APD of $(L-1)N_r$. Note that, for $L=2$, $APD\to N_r$ for all values of $\tilde{n}$.

4) Conclusions: The conclusions drawn in the cases $N_r=1$ and $N_r=2$ can be generalized:

- There is no interest in selecting values of L exceeding 2. While this result contradicts the previously reported findings in the context of RF communications, this finding is related mainly to the full-duplexity and absence of interference in FSO systems where these two unique features clearly distinguish FSO systems from their RF counterparts. In this context, unlike RF multi-hop systems where a single hop is activated in a time slot in order to avoid interference (i.e. one half-duplex node is transmitting and another node is receiving per time slot), all hops can be simultaneously activated in FSO systems where the different highly-directive LOS optical links do not interfere with each other. Consequently, the full-duplex FSO nodes can all transmit, receive or transmit-and-receive in the same time slot with the direct implication of emptying the buffers at a faster pace. Finally, it is worth highlighting that the lack of interest in selecting $L>2$ holds only in the asymptotic regime since this conclusion was reached following from an asymptotic analysis.
- For $L=2$, the position of the bottleneck link does not affect the APD. The choices $\tilde{n}=1$ and $\tilde{n}=N_r+1$ are both optimal since they minimize the OP for the same APD value.
- For $L>2$, the scenario $\tilde{n}=1$ is optimal since it minimizes the OP and APD. The choice $\tilde{n}=N_r+1$ achieves the same optimal OP with the maximum APD.
- It is advisable not to have an intermediate link as the longest hop since this will reduce the diversity advantage of the system.

V. Numerical Results

We next present some numerical results that support the theoretical findings reported in the previous sections. The relays are placed along the line joining S with D and their positions are determined by the vector $\mathbf{d}=(d_1,\ldots,d_{N_r+1})$ with $d_{\text{SD}}=\sum_{n=1}^{N_r+1}d_n$ (all distances will be expressed in km). The corresponding hop distances are taken to range from 1 km to 4 km in coherence with the previous works

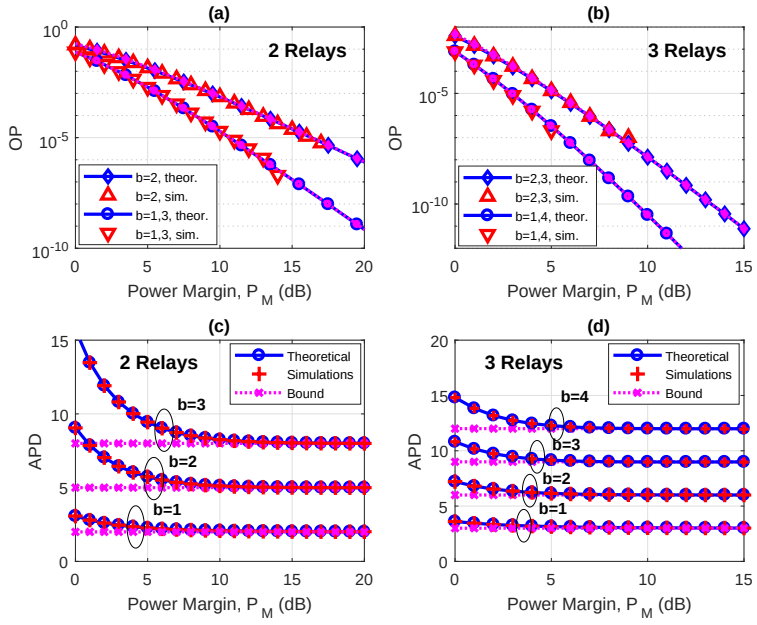

Fig. 5. Performance with 2 and 3 relays for $L = 5$ and $\omega_z/a \to \infty$. The dotted lines correspond to the OP and APD bounds in (36) and (37), respectively. In this figure, $b = \tilde{n}$ indicates the index of the bottleneck hop. Solid lines are used for the theoretical results ("*theor.*") while no lines are used for the simulation results ("*sim.*").

on multi-hop FSO systems [2]–[5]. Regarding the channel parameters, the refractive index structure constant and the attenuation constant are set to $C_n^2 = 1.7 \times 10^{-14}$ m$^{-2/3}$ and $\sigma = 0.44$ dB/km, respectively. The receiver radius (a), beam waist (ω_z) and pointing error displacement standard deviation (σ_s) are assumed to be the same for all hops. In what follows, we set $\sigma_s/a = 3$ while the values of ω_z/a will be varied in the simulations where large values of this ratio indicate less pointing errors. The theoretical OP and APD are determined from the state transition matrix based on equations (20)-(23). In order to check for the validity of the obtained results, the theoretical values are contrasted with their numerical counterparts that are determined from a custom-built discrete event simulator. Results show that the theoretical curves almost perfectly overlap with the numerical curves in all simulated scenarios thus highlighting on the accuracy of the results.

Fig. 3 and Fig. 4 show the performance with one relay for $\omega_z/a = 10$ under the three scenarios $\mathbf{d} = (2.5, 2.5)$, $\mathbf{d} = (2, 3)$ and $\mathbf{d} = (3, 2)$ where, in all scenarios, $d_{\text{SD}=5}$ km. As predicted by the OP expression in (14), the case $L = 1$ presents no diversity advantage where the OP curve is practically parallel to that of buffer-free systems ($L = 0$) in all scenarios. The diversity advantage starts manifesting from $L = 2$ where the increase in the steepness of the OP curves is evident. As expected from (8), scenario 2 and scenario 3 result in the same OP performance for all values of P_M. The asymptotic OP expressions are given in (15) for scenario 1 and in (17) for scenarios 2 and 3. The results in Fig. 3 highlight on the accuracy of these expressions in predicting the system performance starting from relatively small values of P_M. As highlighted in (15), the coding gain enhances with L (for $L \geq 2$) in scenario 1. However, for scenarios 2 and 3, increasing L above 2 does not affect the outage performance where the OP curves are practically the same for $L = 2$ and $L = 5$ in coherence with (17). The corresponding APD values are reported in Fig. 4 where the results highlight on the accuracy of the asymptotic APD expressions provided in (15), (18) and (19) for scenarios 1, 2 and 3, respectively. These simple expressions are useful in predicting the APD values starting from a power margin of 10 dB.

Fig. 5 shows the performance for $d_{\text{SD}} = 6$ km and $L = 5$ with two and three relays in the absence of pointing errors ($\omega_z/a \to \infty$). For $N_r = 2$, we consider the scenarios $\mathbf{d} = (3, 2, 1)$, $\mathbf{d} = (2, 3, 1)$ and $\mathbf{d} = (1, 2, 3)$ corresponding to $\tilde{n} = 1$, $\tilde{n} = 2$ and $\tilde{n} = 3$, respectively. For $N_r = 3$, the following values of $\mathbf{d}$ are simulated: $(2, 1.5, 1.5, 1)$ ($\tilde{n} = 1$), $(1.5, 2, 1.5, 1)$ ($\tilde{n} = 2$), $(1.5, 1.5, 2, 1)$ ($\tilde{n} = 3$) and $(1.5, 1.5, 1, 2)$ ($\tilde{n} = 4$). Results in Fig. 5 show the extremely close match between the theoretical and numerical results whether for the OP curves or for the APD curves. Results in Fig. 5.a and Fig. 5.b highlight on the accuracy of the OP bound in (36) in predicting the asymptotic performance where the achievable diversity order depends on the value of $\hat{n}$. Results in Fig. 5.c and Fig. 5.d highlight on the accuracy of the asymptotic APD expression provided in (37). In particular, the OP bounds are extremely close to the exact values over the entire range of P_M while the APD bounds are close for the values of P_M exceeding 10 dB and 5 dB for $N_r = 2$ and $N_r = 3$, respectively.

Fig. 6 shows the performance with four relays and $\omega_z/a = 8$ for $L = 2$ and $L = 5$. The following scenarios are considered $\mathbf{d} = [4, 2, 2, 2.5, 3]$, $\mathbf{d} = [2, 4, 2.5, 2, 3]$ and $\mathbf{d} = [2, 3, 4, 2, 2.5]$ resulting in $\tilde{n} = 1$, $\tilde{n} = 2$ and $\tilde{n} = 3$, respectively. Results

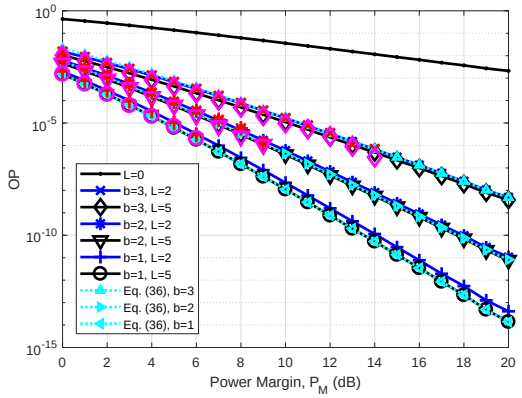

Fig. 6. Performance with 4 relays and $\omega_z/a = 8$ for $L = 2$ and $L = 5$. In this figure, $b = \tilde{n}$ indicates the index of the bottleneck hop. Solid lines are used for the theoretical results, dotted lines for the asymptotic OP in (36) while no lines are used for the simulation results.

validate the theoretical evaluation that matches the numerical analysis and they highlight on the tightness of the OP bound in (36). As highlighted analytically, the asymptotic OP values are practically the same for $L = 2$ and $L = 5$. Results in Fig. 6 also highlight on the remarkable performance gains that can be reaped from equipping the relays with buffers where the gains with respect to buffer-free systems exceed 25 dB at an OP of 10^{-4} for the optimal case $\tilde{n} = 1$. The position of the bottleneck link is also critical on the system performance where, for the same value of the total distance d_{SD}, performance gains in the order of 5.5 dB are observed at an OP of 10^{-5} when comparing the cases $\tilde{n} = 1$ and $\tilde{n} = 3$. These gains increase for decreasing values of the OP following from the enhanced diversity gain that is obtained in the case $\tilde{n} = 1$ compared to the case $\tilde{n} = 3$.

VI. Conclusion

For serial relaying FSO communications, equipping the relays with buffers constitutes a simple and cost-effective solution capable of realizing phenomenal gains in the outage performance. Compared to buffer-free systems, an $(N_r + 1)$-fold increase in the diversity order can be achieved by buffer-aided N_r-relay systems with small buffer sizes not exceeding two. Reaping this maximum diversity advantage inflicts certain conditions on the relay placement where these conditions are clearly delineated through a closed-form asymptotic analysis that relates the system performance to the network parameters in a simple and intuitive manner. The downside of the buffer-aided solution resides in the fact that the packets will arrive at the destination with a delay. However, the delay can be optimized to reach the minimum possible value of N_r time slots where it is judged that this delay falls within acceptable practical limits. While this work targeted an outage analysis, future works should address the consequent appealing problem of evaluating the end-to-end ergodic capacity of serial-relaying buffer-aided FSO systems.

Appendix A

We will solve for the vector π satisfying $\mathbf{A}\pi = \pi$ subject to $\sum_{l=0}^{L} \pi_l = 1$. The relation $\mathbf{A}\pi = \pi$ corresponds to a system of $L + 1$ equations in $L + 1$ unknowns that will be solved recursively.

The first equation (resulting from the first row of $\mathbf{A}$) can be written as $t_{0,0}\pi_0 + t_{1,0}\pi_1 = p_1\pi_0 + p_1(1 - p_2)\pi_1 = \pi_0$ resulting in $\frac{\pi_1}{\pi_0} = \frac{(1-p_1)}{p_1(1-p_2)} = \frac{r}{p_2}$ with $r \triangleq \frac{p_2(1-p_1)}{p_1(1-p_2)}$.

The second equation is given by: $t_{0,1}\pi_0 + t_{1,1}\pi_1 + t_{2,1}\pi_2 = \pi_1$. Replacing the transition probabilities by their values from Section III-A results in:

$$(1-p_1)\pi_0 + [p_1p_2 + (1-p_1)(1-p_2)]\pi_1 + p_1(1-p_2)\pi_2 = \pi_1, \tag{38}$$

where dividing both sides by π_1 while taking into consideration that $\frac{\pi_0}{\pi_1} = \frac{p_2}{r}$ results in $\frac{\pi_2}{\pi_1} = r$.

We will next prove by induction that equations $2, \ldots, L-1$ will result in $\frac{\pi_l}{\pi_{l-1}} = r$ for $l = 2, \ldots, L-1$. From (38), the induction holds for $l = 2$. Assume that it holds for l, we need to prove that it holds for $l + 1$. The $(l + 1)$-th equation of $\mathbf{A}\pi = \pi$ is given by:

$$\underbrace{p_2(1-p_1)}_{t_{l-1,l}}\pi_{l-1} + \underbrace{[p_1p_2 + (1-p_1)(1-p_2)]}_{t_{l,l}}\pi_l + \underbrace{p_1(1-p_2)}_{t_{l+1,l}}\pi_{l+1} = \pi_l, \tag{39}$$

where the transition probabilities are replaced by their values from (5). Dividing both sides of (39) by π_l results in $\frac{\pi_{l+1}}{\pi_l} = r$ since $\frac{\pi_{l-1}}{\pi_l} = \frac{1}{r}$.

The L-th equation can be written as $t_{L-2,L-1}\pi_{L-2} + t_{L-1,L-1}\pi_{L-1} + t_{L,L-1}\pi_L = \pi_{L-1}$. Replacing $t_{L-2,L-1}$ and $t_{L-1,L-1}$ by their values from (5) and $t_{L,L-1}$ by $(1 - p_2)$ results in:

$$p_2(1-p_1)\pi_{L-2} + [p_1p_2 + (1-p_1)(1-p_2)]\pi_{L-1} + (1-p_2)\pi_L = \pi_{L-1}, \tag{40}$$

resulting in $\frac{\pi_L}{\pi_{L-1}} = p_1 r$ since $\frac{\pi_{L-2}}{\pi_{L-1}} = \frac{1}{r}$.

The relations $\frac{\pi_1}{\pi_0} = \frac{r}{p_2}, \frac{\pi_2}{\pi_1} = r, \ldots, \frac{\pi_{L-1}}{\pi_{L-2}} = r, \frac{\pi_L}{\pi_{L-1}} = p_1 r$ result in $\pi_1 = \frac{r}{p_2}\pi_0, \pi_2 = \frac{r^2}{p_2}\pi_0, \ldots, \pi_{L-1} = \frac{r^{L-1}}{p_2}\pi_0, \pi_L = \frac{p_1 r^L}{p_2}\pi_0$ which correspond to the second and third relations in (6). Now, the equation $\sum_{l=0}^{L} \pi_l = 1$ can be written as $\pi_0 \left[1 + \frac{1}{p_2}\sum_{l=1}^{L-1} r^l + \frac{p_1}{p_2}r^L\right] = 1$ whose solution results in the first relation in (6) following from the geometric series sum formula.

Appendix B

Consider first the case $\tilde{n} = 1$; i.e., $\max\{p_1, p_2, p_3\} = p_1$. Since $p_1 \ll 1$, $p_2 \ll 1$ and $p_3 \ll 1$, terms of the form p_n for $n = 2, 3$, $p_n p_{n'}$ for $n, n' = 1, 2, 3$ and $p_1p_2p_3$ will all be neglected compared to p_1. Moreover, the probabilities $1 - p_2$ and $1 - p_3$ will be approximated by 1. Consider the subset of states $\mathcal{S} = \{(0,0), (0,1), (1,0), (1,1)\}$. (i): For $\mathbf{l} = (0,0)$, from case-1 in Section IV-B1, $t_{(0,0),(0,0)} = p_1$ and $t_{(0,0),(1,0)} = 1 - p_1$ and, consequently, transitions from the state $(0,0)$ are all limited towards elements of $\mathcal{S}$. (ii): Consider now the state $\mathbf{l} = (0,1)$. From case-6 in Section

IV-B1, $t_{(0,1),(0,1)} = p_1 p_3 \to 0$, $t_{(0,1),(1,1)} = (1-p_1)p_3 \to 0$, $t_{(0,1),(0,0)} = p_1(1-p_3) \to p_1$ and $t_{(0,1),(1,0)} = (1-p_1)(1-p_3) \to 1-p_1$. Consequently, from the state $(0,1)$, the possible transitions are limited towards the states $(0,0)$ and $(1,0)$ that are both in $\mathcal{S}$. (iii): For $\mathbf{l} = (1,0)$, from case-4 in Section IV-B1, $t_{(1,0),(1,0)} = p_1 p_2 \to 0$, $t_{(1,0),(1,1)} = (1-p_1)(1-p_2) \to 1-p_1$, $t_{(1,0),(2,0)} = (1-p_1)p_2 \to 0$ and $t_{(1,0),(0,1)} = p_1(1-p_2) \to p_1$ implying that the possible transitions are limited towards the elements $(1,1)$ and $(0,1)$ of $\mathcal{S}$. (iv): For $\mathbf{l} = (1,1)$, seven possible transitions can take place according to the probabilities provided in (25). All of the transition probabilities will tend to zero except for the two values $t_{\mathbf{l},\mathbf{l}} \to 1-p_1$ and $t_{\mathbf{l},\mathbf{l}+(-1,0)} \to p_1$ where the transitions $(1,1) \to (1,1)$ and $(1,1) \to (0,1)$ are confined in $\mathcal{S}$.

The proof for $\tilde{n} = 3$ is similar to the case $\tilde{n} = 1$ and, hence, it will be omitted. Consider the case $\tilde{n} = 2$ and the subset $\mathcal{S} = \{(L,0),(L-1,1)\}$. From case-2 in Section IV-B1, $t_{(L,0),(L,0)} = p_2$ and $t_{(L,0),(L-1,1)} = 1-p_2$. Similarly, for $\mathbf{l} = (L-1,1)$, all probabilities in (25) will tend to zero except for $t_{(L-1,1),(L-1,1)} \to 1-p_2$ and $t_{(L-1,1),(L,0)} \to p_2$ proving that $\mathcal{S}$ is a closed-subset.

Appendix C

For $\tilde{n} = 2$, the equation $\mathbf{A}_{\text{red}}^{(2)}[\pi_{(L,0)}, \pi_{(L-1,1)}]^T = [\pi_{(L,0)}, \pi_{(L-1,1)}]^T$ (where $\mathbf{A}_{\text{red}}^{(2)}$ is given in (27)) results in $\pi_{(L,0)} = p_2(\pi_{(L,0)} + \pi_{(L-1,1)}) = p_2$ and $\pi_{(L-1,1)} = (1-p_2)(\pi_{(L,0)} + \pi_{(L-1,1)}) = 1-p_2$ since elements of π' add up to 1.

For $\tilde{n} = 1$ and $\tilde{n} = 3$, from (27), the equation $\mathbf{A}_{\text{red}}^{(\tilde{n})}\pi' = \pi'$ can be easily solved by multiplying both sides of the equation by $\mathbf{A}_{\text{red}}^{(\tilde{n})}$ resulting in $\left[\mathbf{A}_{\text{red}}^{(\tilde{n})}\right]^2 \pi' = \mathbf{A}_{\text{red}}^{(\tilde{n})}\pi' = \pi'$ where (for $\tilde{n} = 1, 3$):

$$\left[\mathbf{A}_{\text{red}}^{(\tilde{n})}\right]^2 = \begin{bmatrix} p_{\tilde{n}}^2 & p_{\tilde{n}}^2 & p_{\tilde{n}}^2 & p_{\tilde{n}}^2 \\ p_{\tilde{n}}(1-p_{\tilde{n}}) & p_{\tilde{n}}(1-p_{\tilde{n}}) & p_{\tilde{n}}(1-p_{\tilde{n}}) & p_{\tilde{n}}(1-p_{\tilde{n}}) \\ p_{\tilde{n}}(1-p_{\tilde{n}}) & p_{\tilde{n}}(1-p_{\tilde{n}}) & p_{\tilde{n}}(1-p_{\tilde{n}}) & p_{\tilde{n}}(1-p_{\tilde{n}}) \\ (1-p_{\tilde{n}})^2 & (1-p_{\tilde{n}})^2 & (1-p_{\tilde{n}})^2 & (1-p_{\tilde{n}})^2 \end{bmatrix}, \tag{41}$$

resulting in the solution given in (28) since elements of π' add up to 1 asymptotically.

Appendix D

Solving for the steady-state distribution will be based on the lumpability method that is applied for the sake of reducing the size of the state space.

Definition *1:* Consider a partition $\{\mathcal{V}_1, \mathcal{V}_2, \ldots\}$ of the state space. The Markov chain is said to be lumpable with respect to this partition if [28, 6.3.2]:

$$\forall\ \mathbf{l_1}, \mathbf{l_2} \in \mathcal{V}_i \ \ ; \ \ t_{\mathbf{l_1},\mathcal{V}_j} = t_{\mathbf{l_2},\mathcal{V}_j}\ \forall\ i \neq j, \tag{42}$$

where $t_{\mathbf{l},\mathcal{V}} \triangleq \sum_{\mathbf{l}' \in \mathcal{V}} t_{\mathbf{l},\mathbf{l}'}$ stands for the transition probability from the state $\mathbf{l}$ to the set $\mathcal{V}$. Theorem [28, 6.3.2] also suggests that the common probability values in (42) constitute the transition probabilities in the lumped chain.

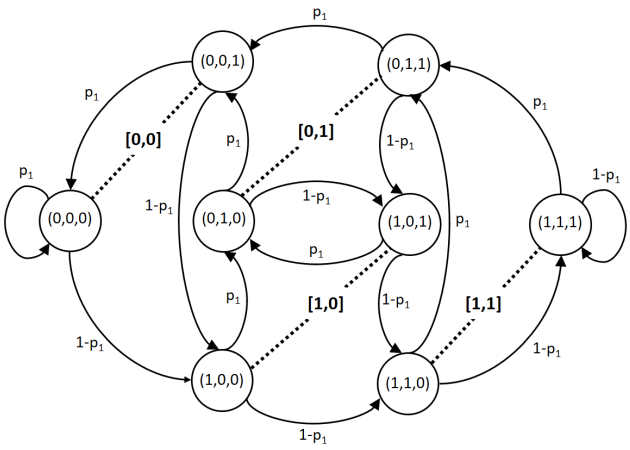

Fig. 7. Lumping of states for $N_r = 3$ and $\tilde{n} = 1$. The states connected by a dashed line will be lumped together. The lumped chain $\{[0,0],[0,1],[1,0],[1,1]\}$ is equivalent to the chain in Fig. 2 with $N_r = 2$ and $\tilde{n} = 1$.

Consider first the case $\tilde{n} = 1$.

Proposition *4:* The transition probabilities of the elements of $\mathcal{S} = \{0,1\}^{N_r}$ are given by:

$$(l_1, \ldots, l_{N_r}) \to \begin{cases} (0, l_1, \ldots, l_{N_r-1}), & p_1; \\ (1, l_1, \ldots, l_{N_r-1}), & 1-p_1. \end{cases}, \tag{43}$$

implying that $\mathcal{S}$ is a closed-subset since $(0, l_1, \ldots, l_{N_r-1})$ and $(1, l_1, \ldots, l_{N_r-1})$ belong to $\mathcal{S}$ whenever $(l_1, \ldots, l_{N_r})$ belongs to $\mathcal{S}$.

Proof: Neglecting the outage events along the non-bottleneck hops, the unavailability probabilities $\{\mathfrak{p}_n\}_{n=2}^{N_r+1}$ in (21) will be equal to either 0 or 1 where $\mathfrak{p}_n = 0$ (resp. $\mathfrak{p}_n = 1$) implies that the n-th hop is available (resp. unavailable).

Consider the transition $(l_1, \ldots, l_{N_r}) \to (l'_1, \ldots, l'_{N_r})$ and an element l_n for $n = 1, \ldots, N_r - 1$. The possible values of (l_n, l_{n+1}) are $\{(0,0),(0,1),(1,0),(1,1)\}$ implying that the corresponding unavailability probabilities $(\mathfrak{p}_{n+1}, \mathfrak{p}_{n+2})$ along the hops preceding and following R_{n+1} are $\{(1,1),(1,0),(0,1),(0,0)\}$ since $l_n = 0 \Rightarrow \mathfrak{p}_{n+1} = 1$ and $l_n = 1 \Rightarrow \mathfrak{p}_{n+1} = 0$. This implies that the corresponding values of l'_{n+1} are $l'_{n+1} = l_{n+1} + \{0,-1,1,0\} = \{0,0,1,1\}$. In fact, in the first and fourth cases the $(n+1)$-th buffer state will remain unchanged since both hops are unavailable and available respectively. In the second (resp. third) case, the preceding link is unavailable (resp. available) while the subsequent hop is available (resp. unavailable) implying that the buffer occupancy will decrease (resp. increase) by 1. It can be observed that in all cases, $l'_{n+1} = l_n$ implying that $(l'_2, \ldots, l'_{N_r}) = (l_1, \ldots, l_{N_r-1})$. Regarding the first hop, $l_1 = 0$ implies that no packets can be forwarded along the second hop resulting in $l'_1 = 0$ with probability p_1 and $l'_1 = 1$ with probability $1-p_1$. Now, $l_1 = 1$ implies that the second hop is available while the unavailability (resp. availability) of the first hop with probability p_1 (resp. $1-p_1$) will incur decreasing the buffer size by one (resp. keeping it unchanged) resulting in $l'_1 = 0$ (resp. $l'_1 = 1$). Combining the above cases results in (43). ■

Observation *1:* The Markov chain with 2^{N_r} states defined over $\mathcal{S}$ is lumpable with respect to the partition of 2^{N_r-1} sets enumerated as $\{\mathcal{V}_{[l_1,\ldots,l_{N_r-1}]}\ ;\ l_1,\ldots,l_{N_r-1}\in\{0,1\}\}$ where:

$$\mathcal{V}_{[l_1,\ldots,l_{N_r-1}]}\triangleq\{(l_1,\ldots,l_{N_r-1},0),(l_1,\ldots,l_{N_r-1},1)\}. \quad (44)$$

Proof: The proof follows directly from (43) where the transitions and their corresponding probabilities are the same whether $l_{N_r}=0$ or $l_{N_r}=1$. More precisely:

$$\begin{aligned} &t_{(l_1,\ldots,l_{N_r-1},i),\mathcal{V}_{[j,l_1,\ldots,l_{N_r-2}]}}\\ &=t_{(l_1,\ldots,l_{N_r-1},i),(j,l_1,\ldots,l_{N_r-2},l_{N_r-1})}\\ &\qquad+\underbrace{t_{(l_1,\ldots,l_{N_r-1},i),(j,l_1,\ldots,l_{N_r-2},\bar{l}_{N_r-1})}}_{=0} \quad (45)\\ &=\begin{cases} p_1, & j=0;\\ 1-p_1, & j=1.\end{cases}\quad;\quad i=0,1, \quad (46)\end{aligned}$$

implying that the transition probabilities are the same for both elements of $\mathcal{V}_{[l_1,\ldots,l_{N_r-1}]}$. In (45), $\bar{l}=0$ if $l=1$ and $\bar{l}=1$ if $l=0$. ∎

Observation *2:* The transition probabilities in the lumped N_r-relay Markov chain are the same as those in the (N_r-1)-relay chain. In other words, the set $\mathcal{V}_{[l_1,\ldots,l_{N_r-1}]}$ is equivalent to the state $(l_1,\ldots,l_{N_r-1})$ in the (N_r-1)-relay chain.

Proof: The proof follows from (46) since:

$$\mathcal{V}_{[l_1,\ldots,l_{N_r-1}]}\rightarrow\begin{cases}\mathcal{V}_{[0,l_1,\ldots,l_{N_r-2}]}, & p_1;\\ \mathcal{V}_{[1,l_1,\ldots,l_{N_r-2}]}, & 1-p_1.\end{cases}, \quad (47)$$

which is equivalent to (43) if N_r is replaced by N_r-1 in this latter equation. ∎

The lumping of states is better clarified in Fig. 7 for $N_r=3$. In what follows, the steady-state distribution will be denoted by $\pi_{\mathbf{l}}^{(N_r,\tilde{n})}$ for an N_r-relay system with the bottleneck hop $\tilde{n}$. Equation (43) can be written as $(l_2,\ldots,l_{N_r},i)\rightarrow(0,l_2,\ldots,l_{N_r})$ with probability p_1 and $(l_2,\ldots,l_{N_r},i)\rightarrow(1,l_2,\ldots,l_{N_r})$ with probability $1-p_1$ resulting in:

$$\begin{aligned}\pi^{(N_r,1)}_{(l_1,l_2,\ldots,l_{N_r})}&=\mathfrak{I}_{l_1}\left[\pi^{(N_r,1)}_{(l_2,\ldots,l_{N_r},0)}+\pi^{(N_r,1)}_{(l_2,\ldots,l_{N_r},1)}\right]\\&=\mathfrak{I}_{l_1}\pi^{(N_r-1,1)}_{(l_2,\ldots,l_{N_r})}, \quad (48)\end{aligned}$$

where $\mathfrak{I}_l\triangleq p_{\tilde{n}}$ if $l=0$ and $\mathfrak{I}_l\triangleq 1-p_{\tilde{n}}$ if $l=1$ and where the second equality follows from observation 2. Applying the relation in (48) recursively $\pi^{(N_r,1)}_{(l_1,l_2,\ldots,l_{N_r})}=\mathfrak{I}_{l_1}\cdots\mathfrak{I}_{l_{N_r-2}}\pi^{(2,1)}_{(l_{N_r-1},l_{N_r})}$ and using the result obtained in (28) in the case of two relays results in (34).

Consider now the case $\tilde{n}-1\leq N_r+1-\tilde{n}$ with $\tilde{n}\neq 1$. The set $\mathcal{S}$ in (33) can be written as:

$$\begin{aligned}\mathcal{S}=\big\{\big(&l^*_{2\tilde{n}-2},\ldots,l^*_{\tilde{n}};l_{\tilde{n}},\ldots,l_{2\tilde{n}-2},l_{2\tilde{n}-1},\ldots,l_{N_r}\big)\\&;\ l_{\tilde{n}},\ldots,l_{N_r}\in\{0,1\}\big\}, \quad (49)\end{aligned}$$

where $l^*=L$ if $l=0$ and $l^*=L-1$ if $l=1$ while the semicolon is used to indicate the position of the bottleneck link.

Proposition *5:* The set $\mathcal{S}$ in (49) is closed since the following transitions are possible:

$$\begin{aligned}&\big(l^*_{2\tilde{n}-2},\ldots,l^*_{\tilde{n}};l_{\tilde{n}},\ldots,l_{2\tilde{n}-2},l_{2\tilde{n}-1},\ldots,l_{N_r}\big)\rightarrow\\&\begin{cases}\big(l^*_{2\tilde{n}-3}\ldots l^*_{\tilde{n}},L;0,l_{\tilde{n}}\ldots l_{2\tilde{n}-3},l_{2\tilde{n}-2}\ldots l_{N_r-1}\big), & p_{\tilde{n}};\\ \big(l^*_{2\tilde{n}-3}\ldots l^*_{\tilde{n}},L-1;1,l_{\tilde{n}}\ldots l_{2\tilde{n}-3},l_{2\tilde{n}-2}\ldots l_{N_r-1}\big), & 1-p_{\tilde{n}}.\end{cases}\end{aligned} \quad (50)$$

where all states in this equation have the structure given in (49) and, hence, they belong to $\mathcal{S}$.

Proof: Consider the transition $(l_1,\ldots,l_{N_r})\rightarrow(l'_1,\ldots,l'_{N_r})$ and an element l_n. Case 1, $\tilde{n}\leq n\leq N_r-1$: The possible values of (l_n,l_{n+1}) are $\{(0,0),(0,1),(1,0),(1,1)\}$ implying that $l'_{n+1}=l_n$ and $(l'_{\tilde{n}+1},\ldots,l'_{N_r})=(l_{\tilde{n}},\ldots,l_{N_r-1})$ following from the proof of proposition 4. Case 2, $1\leq n\leq\tilde{n}-2$: The possible values of (l_n,l_{n+1}) are $\{(L,L),(L,L-1),(L-1,L),(L-1,L-1)\}$ which results in $l'_n=l_{n+1}$ and $(l'_1,\ldots,l'_{\tilde{n}-2})=(l_2,\ldots,l_{\tilde{n}-1})$ where the proof is very similar to that of proposition 4. For example, for $(l_n,l_{n+1})=(L-1,L)$, the link R_n-R_{n+1} is not available while the link R_{n-1}-R_n is available implying that l_n will increase by 1: $l'_n=l_n+1=L=l_{n+1}$. Now consider the values (l_n,l_{n+1}) and their image values with respect to the bottleneck hop $\tilde{n}$ (l_m,l_{m+1}) where $n+m+1=2\tilde{n}-1$. From (49) , $l_m=l^*_{n+1}$ and $l_{m+1}=l^*_n$. Now, from case 1, $l'_{m+1}=l_m=l^*_{n+1}=(l'_n)^*$ where the last equality follows from case 2. Therefore, the structure of the states described in (49) is respected by $(l'_1,\ldots,l'_{N_r})$ at this level (i.e. excluding $l'_{\tilde{n}-1}$ and $l'_{\tilde{n}}$). Case 3, $n=\tilde{n}-1$: The possible values of $(l_{\tilde{n}-1},l_{\tilde{n}})$ are $(L,0)$ and $(L-1,1)$. Now, $(L,0)\rightarrow(L,0)$ and $(L-1,1)\rightarrow(L,0)$ with probability $p_{\tilde{n}}$ where the $\tilde{n}$-th hop is unavailable. In the first case, the hops $\tilde{n}-1$, $\tilde{n}$ and $\tilde{n}+1$ are unavailable implying that the buffer sizes will remain unchanged. In the second case, the hops $\tilde{n}-1$ and $\tilde{n}+1$ are available while the hop $\tilde{n}$ is unavailable implying that the buffer size at $\mathrm{R}_{\tilde{n}-1}$ will increase by 1 while the buffer size at $\mathrm{R}_{\tilde{n}}$ will decrease by 1. Similarly, $(L,0)\rightarrow(L-1,1)$ and $(L-1,1)\rightarrow(L-1,1)$ with probability $1-p_{\tilde{n}}$ completing the proof. ∎

It can be observed that the transition probabilities associated with $(l_1,\ldots,l_{N_r})$ in (50) are the same as the transition probabilities associated with $(l_{\tilde{n}},\ldots,l_{N_r})$ in (43) in an $(N_r-\tilde{n}+1)$-relay system. In fact, the first $\tilde{n}-1$ values of the state $(l_1,\ldots,l_{N_r})$ in (49) are redundant in the sense that they can be determined from the $\tilde{n}-1$ buffer sizes following the bottleneck link. Therefore, the values $l_1,\ldots,l_{\tilde{n}-1}$ just affect the naming of the state without affecting the values of the incoming and outgoing probabilities to and from this state implying that the corresponding Markov chains are equivalent. Consequently, $\pi^{(N_r,\tilde{n})}_{(l_1,\ldots,l_{N_r})}=\pi^{(N_r-\tilde{n}+1,1)}_{(l_{\tilde{n}},\ldots,l_{N_r})}$ which, following from (48), results in the expression given in (34) since only the values $l_{\tilde{n}},\ldots,l_{N_r}$ can be zero.

On the other hand, the proof in the case $\tilde{n}=N_r+1$ is very similar to the case $\tilde{n}=1$ where it can be proven that $t_{(l_1,\ldots,l_{N_r}),(l_2,\ldots,l_{N_r},L)}=p_{\tilde{n}}$ and $t_{(l_1,\ldots,l_{N_r}),(l_2,\ldots,l_{N_r},L-1)}=1-p_{\tilde{n}}$ with the direct consequence that the states $(L,l_2,\ldots,l_{N_r})$ and $(L-1,l_2,\ldots,l_{N_r})$ can be lumped together. In this case, an inverse recursion similar to

the direct recursion provided in (48) will show that the steady-state distribution in the case $\tilde{n} = N_r+1$ is similar to that in the case $\tilde{n} = 1$ by considering the components of $\mathbf{l}$ that are equal to L rather than 0. Finally, the case $N_r + 1 - \tilde{n} \leq \tilde{n} - 1$ with $\tilde{n} \neq N_r+1$ can be handled by ignoring the $N_r-\tilde{n}+1$ elements $l_{\tilde{n}}, \ldots, l_{N_r}$ (that can be computed from $l_{2\tilde{n}-N_r-1}, \ldots, l_{\tilde{n}-1}$) in a way similar to the analysis presented in proposition 5:

$$\pi^{(N_r,\tilde{n})}_{(l_1,\ldots,l_{N_r})} = \pi^{(\tilde{n}-1,\tilde{n})}_{(l_1,\ldots,l_{\tilde{n}-1})} = \mathfrak{I}'_{\tilde{n}-1}\pi^{(\tilde{n}-2,\tilde{n}-1)}_{(l_1,\ldots,l_{\tilde{n}-2})} = \cdots, \quad (51)$$

where $\mathfrak{I}'_l \triangleq p_{\tilde{n}}$ if $l = L$ and $\mathfrak{I}'_l \triangleq 1 - p_{\tilde{n}}$ if $l = L - 1$.

REFERENCES

[1] M. A. Khalighi and M. Uysal, "Survey on free space optical communication: A communication theory perspective," *IEEE communications surveys & tutorials*, vol. 16, no. 4, pp. 2231–2258, Nov. 2014.

[2] M. Safari, M. Rad, and M. Uysal, "Multi-hop relaying over the atmospheric poisson channel: Outage analysis and optimization," *IEEE Trans. Commun.*, vol. 60, no. 3, pp. 817 –829, March 2012.

[3] S. Kazemlou, S. Hranilovic, and S. Kumar, "All-optical multihop free-space optical communication systems," *J. Lightwave Technol.*, vol. 29, no. 18, pp. 2663 – 2669, September 2011.

[4] C. Abou-Rjeily, "Power allocation for quantum-limited multihop free-space optical communication systems," *IEEE Commun. Lett.*, vol. 16, no. 12, pp. 2068–2071, December 2012.

[5] S. M. Aghajanzadeh and M. Uysal, "Multi-hop coherent free-space optical communications over atmospheric turbulence channels," *IEEE Trans. Commun.*, vol. 59, no. 6, pp. 1657 – 1663, June 2011.

[6] I. Krikidis, T. Charalambous, and J. S. Thompson, "Buffer-aided relay selection for cooperative diversity systems without delay constraints," *IEEE Trans. Wireless Commun.*, vol. 11, no. 5, pp. 1957–1967, May 2012.

[7] Z. Tian, G. Chen, Y. Gong, Z. Chen, and J. A. Chambers, "Buffer-aided max-link relay selection in amplify-and-forward cooperative networks," *IEEE Trans. Veh. Technol.*, vol. 64, no. 2, pp. 553–565, Feb. 2015.

[8] Z. Tian, Y. Gong, G. Chen, and J. Chambers, "Buffer-aided relay selection with reduced packet delay in cooperative networks," *IEEE Trans. Veh. Technol.*, vol. 66, no. 3, pp. 2567–2575, Mar. 2017.

[9] B. Manoj, R. K. Mallik, and M. R. Bhatnagar, "Performance analysis of buffer-aided priority-based max-link relay selection in DF cooperative networks," *IEEE Trans. Commun.*, vol. PP, no. 99, pp. 1–1, Oct. 2018.

[10] A. A. M. Siddig and M. F. M. Salleh, "Buffer-aided relay selection for cooperative relay networks with certain information rates and delay bounds," *IEEE Trans. Veh. Technol.*, vol. 66, no. 11, pp. 10 499–10 514, Nov. 2017.

[11] T. Charalambous, N. Nomikos, I. Krikidis, D. Vouyioukas, and M. Johansson, "Modeling buffer-aided relay selection in networks with direct transmission capability," *IEEE Commun. Lett.*, vol. 19, no. 4, pp. 649–652, Apr. 2015.

[12] D. Q. Qiao and M. C. Gursoy, "Buffer-aided relay systems under delay constraints: Potentials and challenges," *IEEE Communications Magazine*, vol. 55, no. 9, pp. 168–174, Sep. 2017.

[13] N. Nomikos, T. Charalambous, D. Vouyioukas, and G. K. Karagiannidis, "Low-complexity buffer-aided link selection with outdated CSI and feedback errors," *IEEE Trans. Commun.*, Mar. 2018.

[14] L.-L. Yang, C. Dong, and L. Hanzo, "Multihop diversity-a precious source of fading mitigation in multihop wireless networks," in *IEEE Global Telecommun. Conf. (GLOBECOM)*, Dec. 2011, pp. 1–5.

[15] C. Dong, L.-L. Yang, and L. Hanzo, "Performance analysis of multihop-diversity-aided multihop links," *IEEE Trans. Veh. Technol.*, vol. 61, no. 6, pp. 2504–2516, July 2012.

[16] V. Jamali, N. Zlatanov, H. Shoukry, and R. Schober, "Achievable rate of the half-duplex multi-hop buffer-aided relay channel with block fading," *IEEE Trans. Wireless Commun.*, vol. 14, no. 11, pp. 6240–6256, Nov. 2015.

[17] M. M. Razlighi and N. Zlatanov, "Buffer-aided relaying for the two-hop full-duplex relay channel with self-interference," *IEEE Trans. Wireless Commun.*, vol. 17, no. 1, pp. 477–491, Jan. 2018.

[18] V. Jamali, D. S. Michalopoulos, M. Uysal, and R. Schober, "Link allocation for multiuser systems with hybrid RF/FSO backhaul: Delay-limited and delay-tolerant designs," *IEEE Trans. Wireless Commun.*, vol. 15, no. 5, pp. 3281–3295, May 2016.

[19] Y. F. Al-Eryani, A. M. Salhab, S. A. Zummo, and M.-S. Alouini, "Protocol design and performance analysis of multiuser mixed RF and hybrid FSO/RF relaying with buffers," *IEEE/OSA Journal of Opt. Commun. and Netw.*, vol. 10, no. 4, pp. 309–321, Apr. 2018.

[20] M. Najafi, V. Jamali, and R. Schober, "Optimal relay selection for the parallel hybrid RF/FSO relay channel: Non-buffer-aided and buffer-aided designs," *IEEE Trans. Commun.*, vol. 7, no. 65, pp. 2794–2810, April 2017.

[21] C. Abou-Rjeily and W. Fawaz, "Buffer-aided relaying protocols for cooperative FSO communications," *IEEE Trans. Wireless Commun.*, vol. 16, no. 12, pp. 8205–8219, Dec. 2017.

[22] A. Farid and S. Hranilovic, "Outage capacity optimization for free-space optical links with pointing errors," *J. Lightwave Technol.*, vol. 25, no. 7, pp. 1702–1710, July 2007.

[23] H. Sandalidis, T. Tsiftsis, and G. Karagiannidis, "Optical wireless communications with heterodyne detection over turbulence channels with pointing errors," *J. Lightwave Technol.*, vol. 27, no. 20, pp. 4440–4445, October 2009.

[24] C. Abou-Rjeily and Z. Noun, "Impact of inter-relay cooperation on the performance of FSO systems with any number of relays," *IEEE Trans. Wireless Commun.*, vol. 15, no. 6, pp. 3796–3809, June 2016.

[25] N. D. Chatzidiamantis, D. S. Michalopoulos, E. E. Kriezis, G. K. Karagiannidis, and R. Schober, "Relay selection protocols for relay-assisted free-space optical systems," *IEEE J. Opt. Commun. Netw.*, vol. 5, no. 1, pp. 4790 –4807, January 2013.

[26] J. D. C. Little and S. C. Graves, "Little's law," in *International Series in Operations Research & Management Science*, New York, NY, USA: Springer-Verlag, vol. 115, pp. 81–100, 2008.

[27] W. J. Stewart, *Probability, Markov chains, queues, and simulation: the mathematical basis of performance modeling*. Princeton University Press, July 2009.

[28] J. G. Kemeny and J. L. Snell, *Finite markov chains*. D. Van Nostrand, Princeton, New Jersey, 1960.